

NASA TECHNICAL NOTE



NASA TN D-4515

2.1

NASA TN D-4515



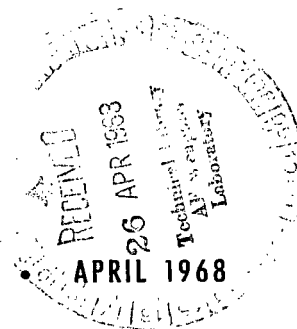
LOAN COPY: RETURN TO
AFWL (WLIL-2)
KIRTLAND AFB, N MEX

STABILIZING EFFECTS OF
SEVERAL INJECTOR FACE BAFFLE
CONFIGURATIONS ON SCREECH
IN A 20 000-POUND-THRUST
HYDROGEN-OXYGEN ROCKET

by Ned P. Hannum, Harry E. Bloomer, and Ralph R. Goelz

*Lewis Research Center
Cleveland, Ohio*

NATIONAL AERONAUTICS AND SPACE ADMINISTRATION • WASHINGTON, D. C.





STABILIZING EFFECTS OF SEVERAL INJECTOR FACE BAFFLE
CONFIGURATIONS ON SCREECH IN A 20 000-POUND-THRUST
HYDROGEN-OXYGEN ROCKET

By Ned P. Hannum, Harry E. Bloomer, and Ralph R. Goelz

Lewis Research Center
Cleveland, Ohio

NATIONAL AERONAUTICS AND SPACE ADMINISTRATION

For sale by the Clearinghouse for Federal Scientific and Technical Information
Springfield, Virginia 22151 - CFSTI price \$3.00

STABILIZING EFFECTS OF SEVERAL INJECTOR FACE BAFFLE CONFIGURATIONS ON SCREECH IN A 20 000-POUND-THRUST HYDROGEN- OXYGEN ROCKET

by Ned P. Hannum, Harry E. Bloomer, and Ralph R. Goelz
Lewis Research Center

SUMMARY

Experimental tests were conducted at the Lewis Research Center to assess the worth of injector face baffles as screech suppression devices. Seventeen injector face baffle configurations were evaluated with 94 hot firings. The number of injector face baffle compartments was varied from 3 to 100 with lengths from 1/2 to 2 inches (1.3 to 5.1 cm).

Stability data were obtained at a chamber pressure of 300 pounds per square inch (2070 kN/sq m) absolute and over a range of oxidant-fuel ratios of from 4 to 6. Hydrogen injection temperature was used to rate the stability of the various baffles. The baffle with the lowest self-triggering temperature was considered to be the most stable.

The results indicate that injector face baffles 2 inches (5.1 cm) long produced acoustic stability to the minimum hydrogen injection temperature limit of the test facility (55° R or 31° K) with maximum compartment dimensions as large as 9.1 inches (23.1 cm). Acoustic stability down to a hydrogen injection temperature of 55° R (31° K) could also be achieved with injector face baffles 1 inch (2.5 cm) in length when the maximum compartment dimension was less than 4 inches (10.2 cm). One of the configurations was, however, only marginally stable at the reduced temperature.

INTRODUCTION

The size of the combustion chambers of liquid propellant rockets has, by necessity, been increasing over the past several years. The result has been increased occurrences of an acoustic mode combustion instability commonly referred to as "screech". The rocket industry has conducted extensive experimental and analytical research into the nature and prevention of screech. Years ago, the industry discovered that screech could

often be eliminated by the installation of injector face baffles. Several explanations of baffle effectiveness have been hypothesized as follows:

- (1) Decoupling the combustion zone geometry and the combustion process by compartmentalizing the combustion zone to smaller dimensions and consequently increasing the natural frequency of the combustion zone (refs. 1 and 2)
- (2) Increasing the viscous losses by adding more surface area and consequently increasing the acoustic damping rate (ref. 3)
- (3) Reducing the cross velocity effect on the local mixture ratio (ref. 4)
- (4) Obstructing acoustic paths in the combustor (refs. 3 and 4)

As part of a comprehensive program at the Lewis Research Center to investigate causes and cures for high-frequency combustion instability, several injector face baffle configurations were tested to assess their worth as screech-suppression devices. Baffles were designed to evaluate any trade off between length and number of baffle compartments. The investigation was conducted in a rocket engine test facility at Lewis, using a hydrogen-oxygen rocket engine 10.77 inches (27.4 cm) in diameter. The engine was operated at a chamber pressure of 300 pounds per square inch (2070 kN/sq m) and produced a sea-level thrust of 20 000 pounds (9070 kg), the equivalent of 28 000 pounds (12 700 kg) in a vacuum with a 40-to-1 exhaust nozzle. The temperature rating technique described in reference 5 was used to screech rate each configuration. The injector face baffle lengths varied from 1/2 to 2 inches (1.3 to 5.1 cm). The number of baffle compartments varied from 3 to approximately 100. The injector used for these tests had a strong tendency to screech and therefore provided a critical test configuration (ref. 5).

APPARATUS

Test Facility

The Rocket Engine Test Facility, used for this investigation, is a 50 000-pound-thrust (22 680-kg-thrust) sea-level stand equipped with an exhaust gas muffler and scrubber. The facility used a pressurized propellant system to deliver the propellants to the engine from the storage tanks. The oxygen propellant line and storage tank were immersed in a liquid nitrogen bath. The liquid hydrogen line was insulated with a plastic-type foam. Gaseous hydrogen was stored at ambient temperature and delivered to the test stand in uninsulated lines. A more detailed description of the engine test stand and the facility may be found in reference 5.

Engine

The rocket engine (fig. 1) was comprised of a concentric tube injector, a cylindrical heat-sink thrust chamber of 10.77 inch (27.4 cm) inside diameter, and a convergent-divergent heat-sink exhaust nozzle with a contraction ratio of 1.90 and an expansion area ratio of 1.30. The length of the thrust chamber was 17.94 inches (45.6 cm). The inner surfaces of the mild-steel heat-sink thrust chamber and nozzle were flame spray coated with 0.012 inch (0.030 cm) of nickel chromium beneath 0.018 inch (0.046 cm) of zirconium oxide to reduce the rate of heat transfer to the metal. This allowed a run duration of 3 seconds which was adequate for the test.

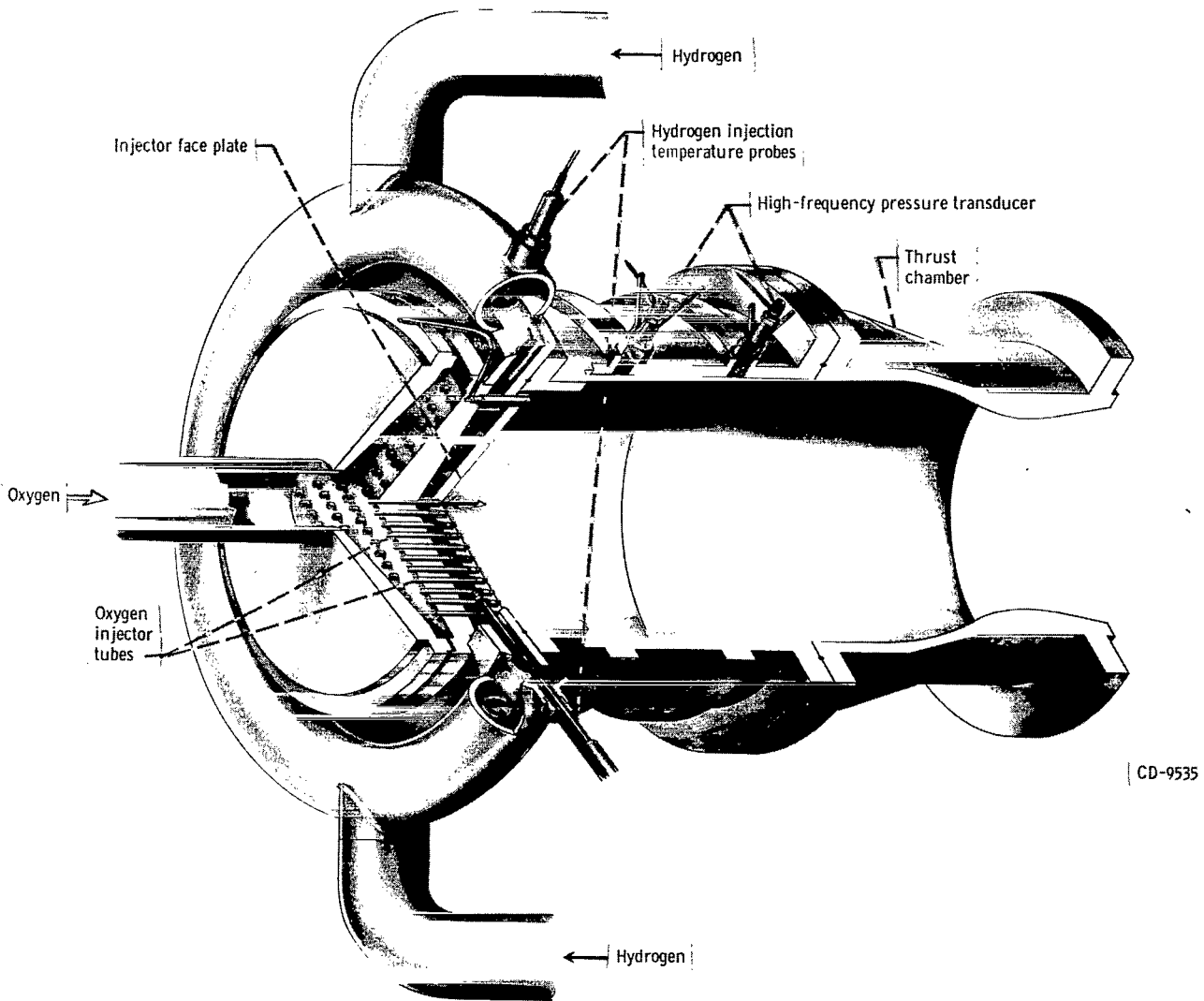


Figure 1. - Engine and injector.

Injector

The removable faceplate of the 421-element injector was fabricated from 1/2-inch-thick (1.3-cm-thick) copper. In an attempt to prevent torching of the leading edges of the various baffle configurations, the injectors were modified by plugging selected elements as listed in table I and sketched in figure 2.

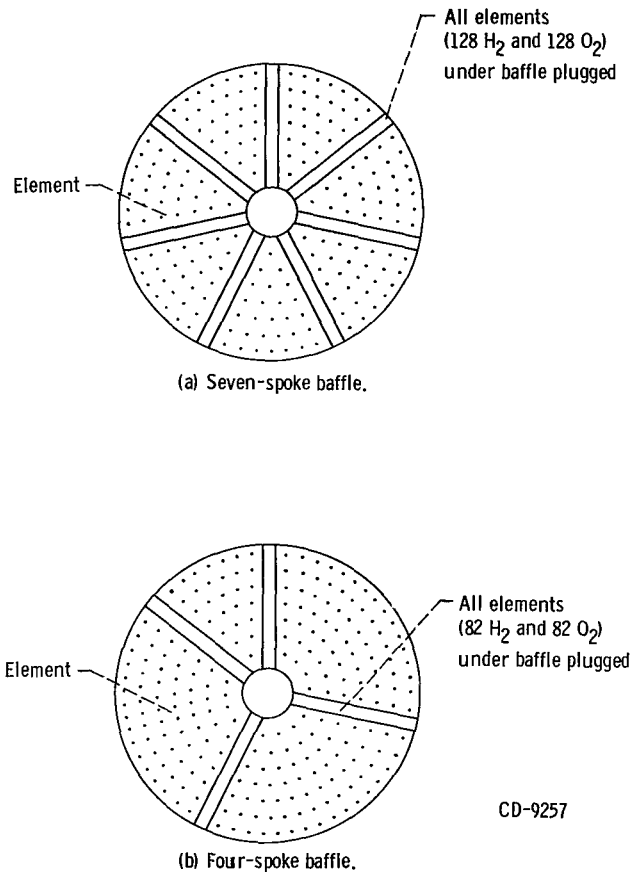
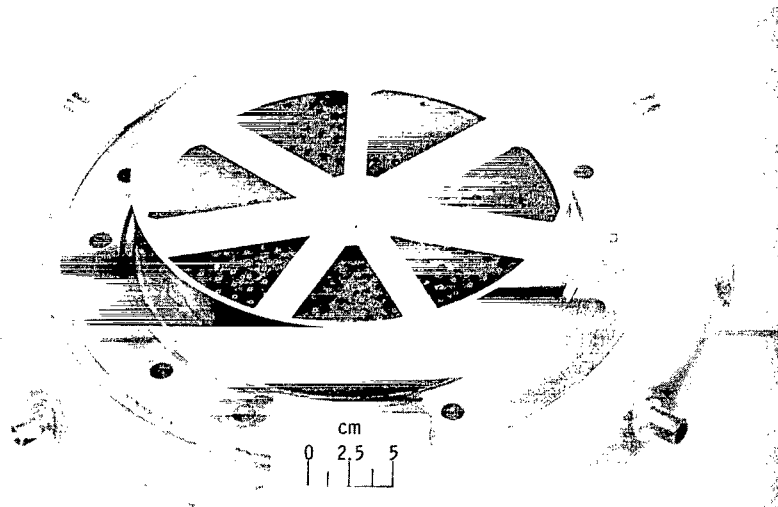


Figure 2. - Injector modifications.

Baffle Configuration

The baffles, pictured in figure 3, were constructed of mild steel and were flame spray coated with 0.012-inch (0.030-cm) nickel chromium under 0.018-inch-thick (0.046-cm-thick) zirconium oxide. These coatings were used to reduce the rate of heat transfer into the metal. A summary of the configurations and the lengths tested is shown in table II. No attempt was made to seal the baffles to either the injector face or the chamber wall. The result was a gap between the injector face and the baffle and



C-72982

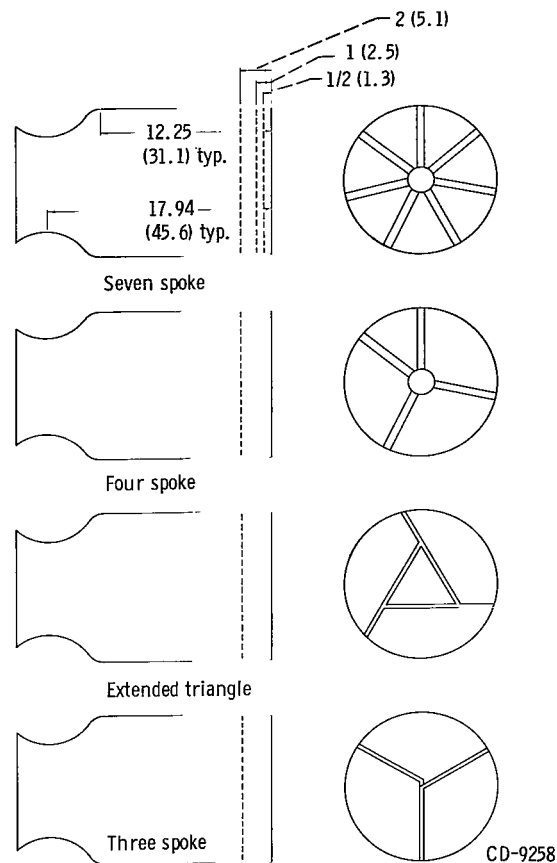
(a) 1-Inch-long (2.5-cm-long) seven-spoke baffle with injector.



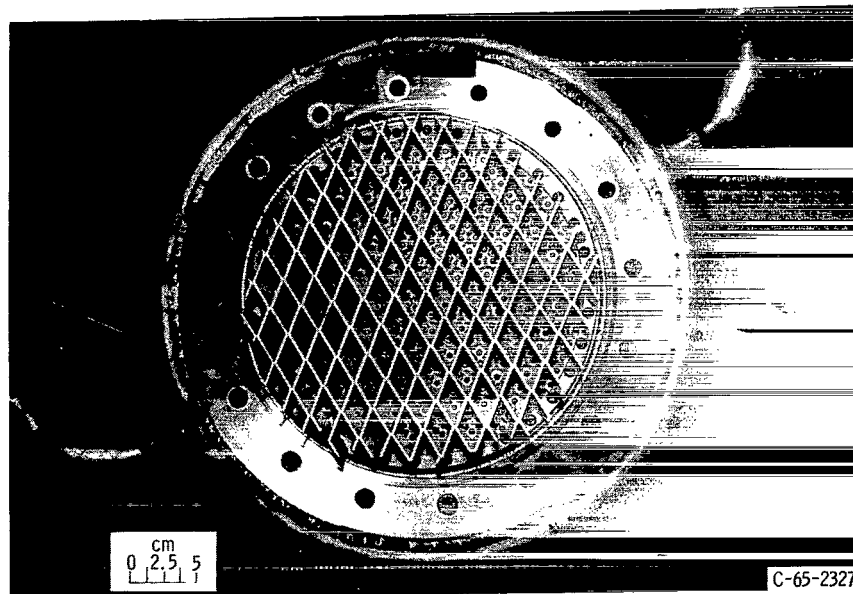
C-65-943

(b) 2-Inch-long (5.1-cm-long) extended triangle baffle with injector.

Figure 3. - Baffle configurations. (All dimensions in inches (and centimeters) unless indicated otherwise.)

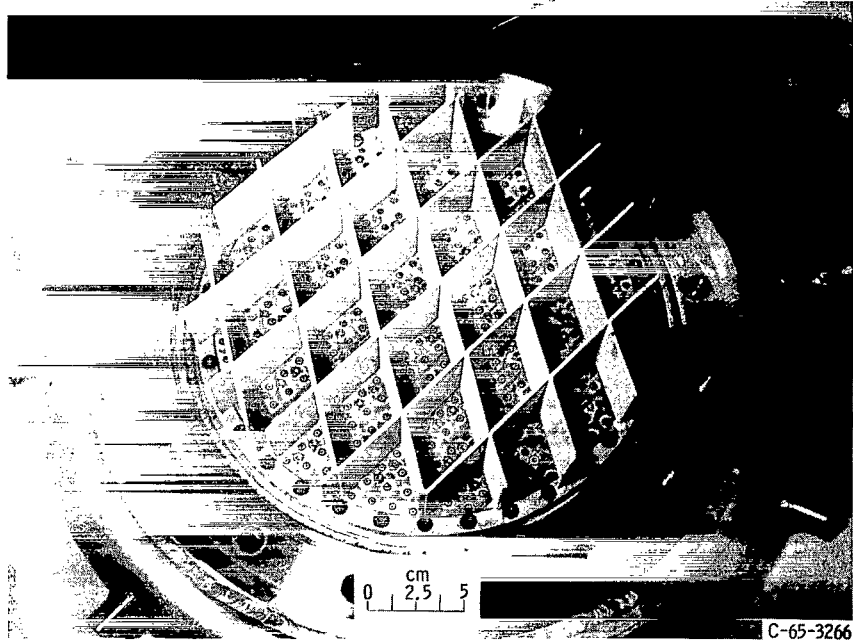


(c) Four injector face baffle configurations.

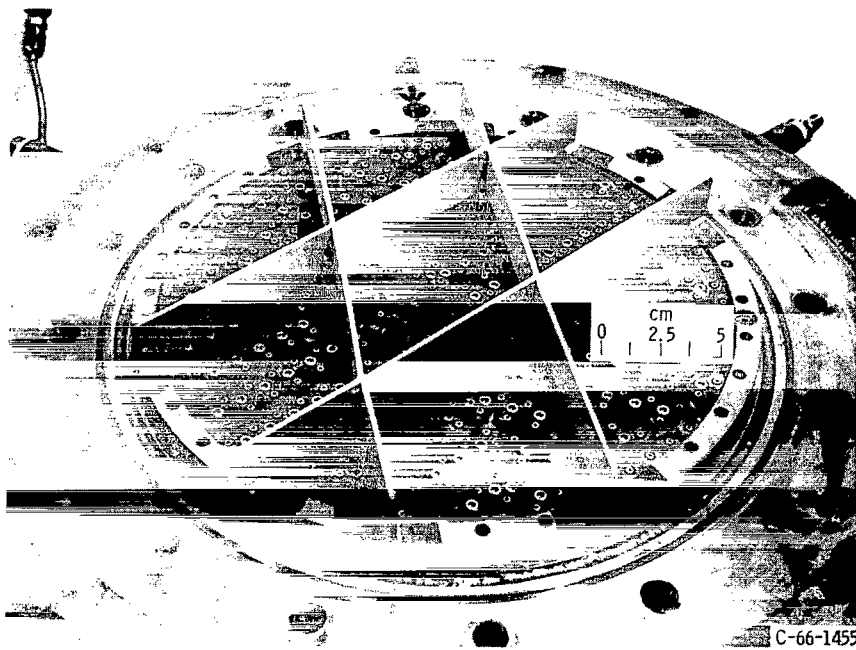


(d) 2-Inch-long (5.1-cm-long) 100-compartment egg-grate baffle with injector.

Figure 3. - Continued.



(e) 2-Inch-long (5.1-cm-long) 25-compartment egg-crate baffle with injector.



(f) 1-Inch-long (2.5-cm-long) seven-compartment egg-crate baffle with injector.

Figure 3. - Concluded.

between the chamber wall and the baffle. This gap, however, did not exceed 0.1 inch (0.25 cm) with any of the baffles. Effects of gap on stability have been reported by Senneff (ref. 6) with earth-storable propellants. Propellant accumulating in the gaps was believed to be "popping" and triggering combustion instability. Popping usually occurred when the gap exceeded 0.3 inch (0.76 cm).

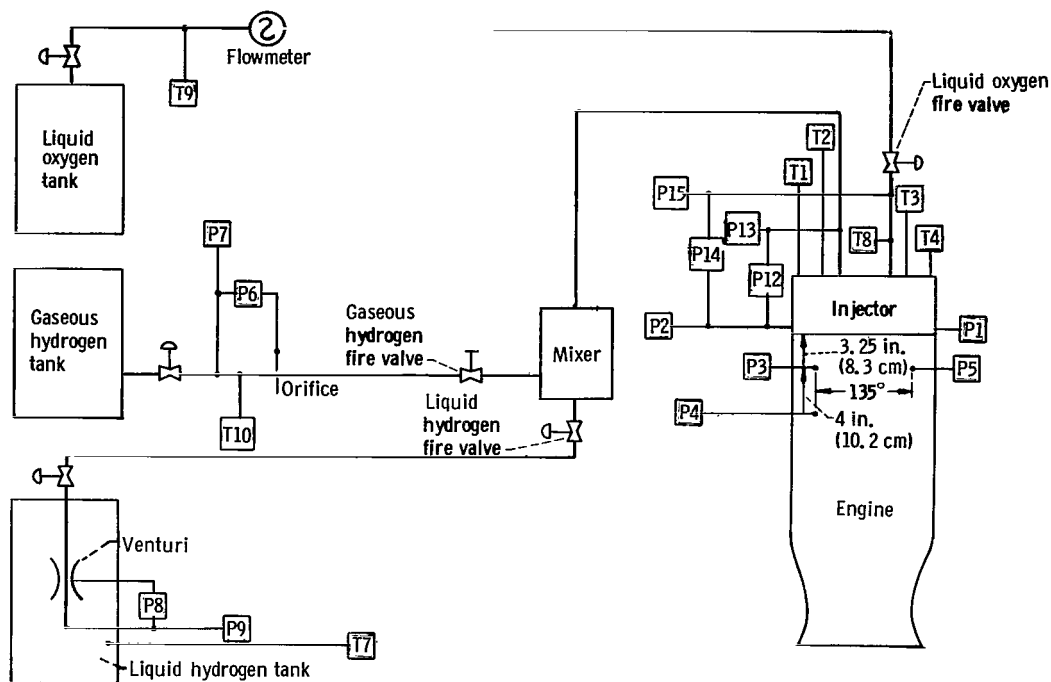
Hydrogen Temperature Controller

The hydrogen temperature ramp used to determine the screech limits was accomplished by varying the amount of 50° R (28° K) liquid hydrogen and ambient temperature gaseous hydrogen in the mixing tube while maintaining a constant flow rate. Mixing was accomplished by swirling the liquid into the gaseous hydrogen stream. The mixing section was 4 feet (122.4 cm) long and was located just upstream of the injector. A constant mixture ratio was maintained by the automatic controller by adjusting the flow rate of the liquid hydrogen while the gaseous hydrogen flow rate was continuously decreased.

INSTRUMENTATION

Locations for the various transducers are shown in a schematic diagram of the engine and associated plumbing (fig. 4). Signals from the transducers were transmitted on land lines to the control room and to the Center's automatic digital data recording system. Piezoelectric-type, water-cooled, flush-mounted pressure transducers were used at three locations on the thrust chamber (see fig. 4) to determine the character and phase relationship of the pressure field and allow identification of the screech mode. The natural frequency of the transducer was 20 000 hertz. The response characteristics of the transducers are flat to within 10 percent to a frequency of 6000 hertz when mounted. The signals from high-frequency response transducers were recorded in analog form on magnetic tape and, in addition, were displayed on direct reading instruments for visual monitoring during the tests.

Oxygen propellant flow rate was determined with a vane-type flowmeter which was calibrated with water using a static weighing system. The flowmeter manufacturer supplied the correction from water calibration to cryogenic calibration. Liquid hydrogen flow rate was measured using a venturi submerged in the liquid hydrogen tank, and the gaseous hydrogen flow rate was measured using an orifice plate. The strain-gage-type pressure transducers were calibrated against a commercial standard. The liquid flow temperatures were measured by platinum resistance-type sensors described in reference 7. The hydrogen injection temperature was measured using four carbon resistance-type probes (ref. 8) that were installed as illustrated in figure 1.



- | | | | |
|-----|---|-----|--|
| P1 | Static chamber pressure (injector face), four-arm strain-gage transducer 1 | P13 | Hydrogen injector pressure, four-arm strain-gage transducer |
| P2 | Static chamber pressure (injector face), four-arm strain-gage transducer 2 | P14 | Oxygen injector differential pressure, four-arm strain-gage transducer |
| P3 | Dynamic chamber pressure, water-cooled quartz pressure transducer 3 | P15 | Oxygen injector pressure, four-arm strain-gage transducer |
| P4 | Dynamic chamber pressure, water-cooled quartz pressure transducer 4 | T1 | Hydrogen injector temperature, carbon resistor sensor probe 1 |
| P5 | Dynamic chamber pressure, water-cooled quartz pressure transducer 5 | T2 | Hydrogen injector temperature, carbon resistor sensor probe 2 |
| P6 | Gaseous hydrogen orifice differential pressure, four-arm strain-gage transducer | T3 | Hydrogen injector temperature, carbon resistor sensor probe 3 |
| P7 | Gaseous hydrogen orifice pressure, four-arm strain-gage transducer | T4 | Hydrogen injector temperature, carbon resistor sensor probe 4 |
| P8 | Liquid hydrogen venturi differential pressure, four-arm strain-gage transducer | T7 | Liquid hydrogen venturi temperature, platinum resistor sensor probe |
| P9 | Liquid hydrogen venturi pressure, four-arm strain-gage transducer | T8 | Oxygen injector temperature, copper-constantan thermocouple |
| P12 | Hydrogen injector differential pressure, four-arm strain-gage transducer | T9 | Oxygen flowmeter temperature, platinum resistor sensor |
| | | T10 | Gaseous hydrogen orifice temperature, iron-constantan thermocouple |

Figure 4. - Instrumentation diagram.

PROCEDURE

As mentioned in the INTRODUCTION, the stability rating of each configuration was expressed in terms of the hydrogen temperature at which screech was encountered (ref. 5). The technique employed was to ramp the hydrogen injection temperature downward to initially probe for the temperature of transition to screech. Ramp rates up to 50°R (28°K) per second were possible for this type of operation with only small variations in the oxidant-fuel ratio. If by the initial ramping technique the configuration was stable to the minimum hydrogen injection temperature available with the facility, subsequent tests were made using only the liquid hydrogen at approximately 50°R (28°K). The screech limit was defined as the instantaneous hydrogen injection temperature corresponding to the initiation of high-frequency pressure oscillations with an amplitude greater than the noise level of stable combustion. Data were obtained over a range of oxidant-fuel ratios to establish a stability limit curve.

Figure 5 shows a typical time history of hydrogen injection temperature, high-frequency chamber pressure, static chamber pressure, and propellant flow rates. The step changes in the run marker correspond to signals to open and then close the oxidizer fire valve. Combustion instability for the example shown was encountered at a hydrogen injection temperature of 70°R (39°K).

Association of the oscillatory pressures with instability mode was tried by compar-

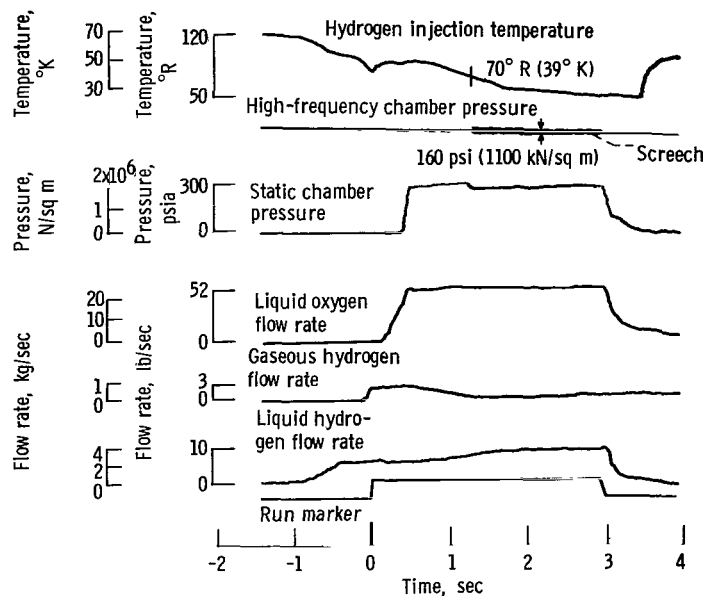


Figure 5. - Oscillograph traces of typical screech test illustrating hydrogen temperature rating technique.

ing the measured acoustic frequencies with the predicted acoustic frequencies. The high-frequency transducers used to obtain the data were located downstream of even the longest baffles and, therefore, would probably not respond to any higher-frequency compartment modes. Consequently, comparisons of screech modes were made using a standard unbaffled combustion chamber as a basis. The frequencies of several screech modes for the combustion chamber geometry used are presented in figure 6 as a function of oxidant-fuel ratio and characteristic exhaust velocity efficiency. The lowest calculated frequency mode is first longitudinal. The frequency is 2050 hertz at an oxidant-fuel ratio of 4 and decreases to 1860 hertz at an oxidant-fuel ratio of 6 for a combustion efficiency of 100 percent. A decrease in characteristic exhaust velocity efficiency will reduce the frequency of a mode by a proportional amount. For an oxidant-fuel ratio range of 4 to 6 and 100 percent combustion efficiency, the range of frequency of the first tangential mode is 3680 to 3340 hertz and the frequency range of the first radial mode is 7500 to 6800 hertz (fig. 6). Mode identification by frequency alone is difficult for frequencies greater than 5000 hertz.

The recorded signals from the high-frequency pressure transducers were analyzed using a heterodyne technique to produce amplitude spectral density curves. The frequency range of 0 to 10 000 hertz was scanned 20 times per second, producing spectral lines at 40-hertz intervals. In a rocket engine, the shape of a pressure wave is non-sinusoidal (ref. 9); as a result, Fourier harmonics may be present in the frequency

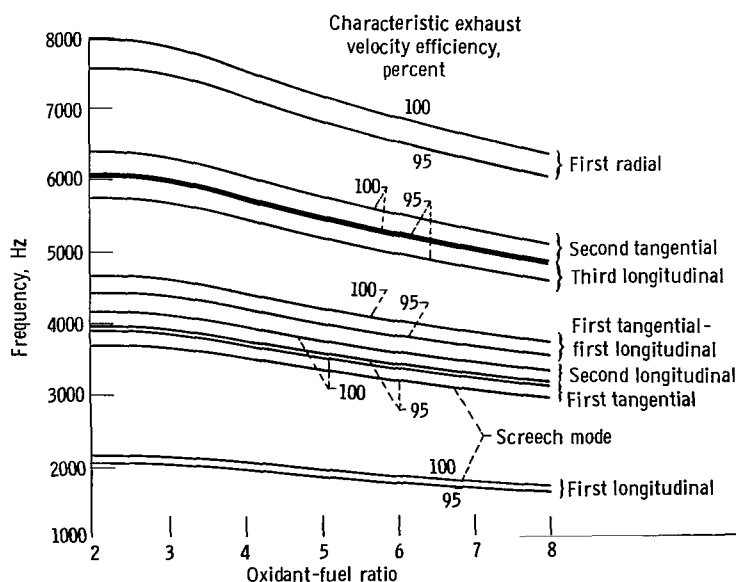


Figure 6. - Effect of oxidant-fuel ratio and characteristic exhaust velocity efficiency on frequency of several modes of screech.

spectrum. In addition, screech may occur in higher-order modes or combined modes of the predominant first transverse or first longitudinal. The frequencies of higher-order transverse or combined modes are not exact multiples of the predominant frequency. The curved walls of the chamber cause the path lengths to be less than exact multiples of the path length of the corresponding predominant mode. Consequently, spectral lines that occurred at exact frequency multiples were identified as Fourier harmonics and were not considered as modes of screech.

METHODS OF CALCULATION

Determination of an accurate value of the instantaneous hydrogen flow rate from the injector at the time of screech inception was difficult because of the nature of the temperature ramping technique. Mass accumulation due to a large change in hydrogen density with temperature during a temperature ramp run occurred between the flow measuring stations (liquid and gas) and the injector face. Despite strenuous efforts to account for this source of error, the oxidant-fuel ratios shown in later figures are undoubtedly subject to scatter and some error in mean value.

Characteristic exhaust velocity efficiency was used as a measure of combustion performance. The chamber pressure used in determining the experimental characteristic exhaust velocity was corrected for momentum pressure loss by the method described in reference 10. Theoretical characteristic exhaust velocity (equilibrium composition) was obtained from reference 11.

RESULTS AND DISCUSSION

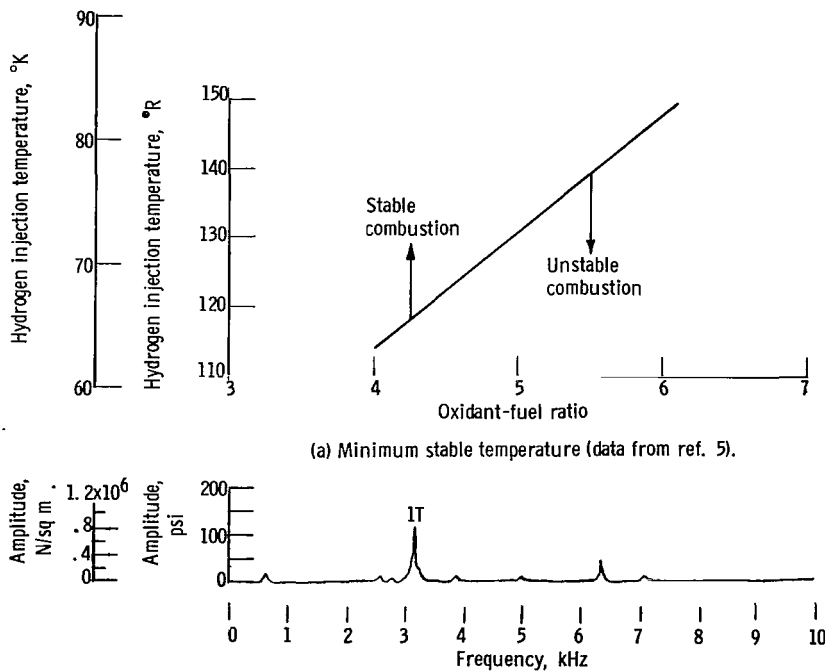
In this investigation, hydrogen injection temperature was used to rate the screech stability characteristics of several injector face baffles. The baffle with the lowest self-triggering temperature was considered the most stable. The effect of baffle length on combustion stability in seven different designs will be presented, followed by a discussion of the effects of baffles on combustion performance. All of the stability data are then summarized by presenting a correlating parameter. Table III presents a tabulation of the data.

A low frequency was present during the operation of some of the injector face baffle configurations. Although an analysis of the low-frequency instabilities was not a part of this investigation, reference 12 describes an entropy wave instability type with a frequency in the range of 330 to 420 hertz for this chamber geometry. Another common instability type is chugging. Frequency predictions for this instability type are difficult

because there are many possible solutions to the double-deal-time model (ref. 13), but generally the frequency will be less than 500 hertz. No assumptions are made as to the effect of these low-frequency instabilities on the prevention or initiation of screech. However, reference 14 has shown that chugging may reduce the combustion performance.

Stability Characteristics of Basic Nonbaffled Configuration

The basic injector-chamber configuration used for evaluation of the various injector face baffle designs was previously reported (ref. 5) to have the stability characteristics shown in figure 7. The minimum stable hydrogen injection temperature is presented as a function of oxidant-fuel ratio and is shown to be 130°R (72°K) at 5.0 (fig. 7(a)). The amplitude spectral density during unstable operation indicated a predominant frequency of 3200 hertz at an amplitude of 120 pounds per square inch (830 kN/sq m) peak-to-peak (fig. 7(b)), which corresponds to the first tangential acoustic mode. Figure 7(b) also shows the first Fourier harmonic at 6400 hertz.



(a) Minimum stable temperature (data from ref. 5).
(b) Amplitude spectral density. Unstable combustion; oxidant-fuel ratio, 6.51; characteristic exhaust velocity efficiency, 94.3 percent; amplitude, peak to peak.

Figure 7. - Stability characteristics of basic configuration used for evaluation of several injector face baffle designs.

Effect of Baffle Length with Three-Spoke and Extended Triangle

The 2-inch-long (5.1-cm-long) extended triangle configuration (figs. 3(b) and (c)) was found to be stable down to the minimum temperature limit of the facility. Tests were conducted at oxidant-fuel ratios of 3.5 and 4.12 (fig. 8).

The three-spoke configuration (fig. 3(c)) was also operated with a 2 inch (5.1 cm) length and found to be stable down to the temperature limit of the facility (fig. 8). An additional data point was obtained, however, during the last test with this configuration. Instability was encountered at 63° R (35° K) and an oxidant-fuel ratio of 3.1. Inspection of the baffle after this run revealed that the baffle had burned back to an average length of approximately 1.6 inches (4.1 cm) (fig. 9). Operation with the shortened baffle resulted in high-frequency oscillations at 7000 and 7800 hertz and amplitudes of approximately 55 pounds per square inch (380 kN/sq m) peak-to-peak (fig. 10). These frequencies are too high for mode identification from frequency considerations alone.

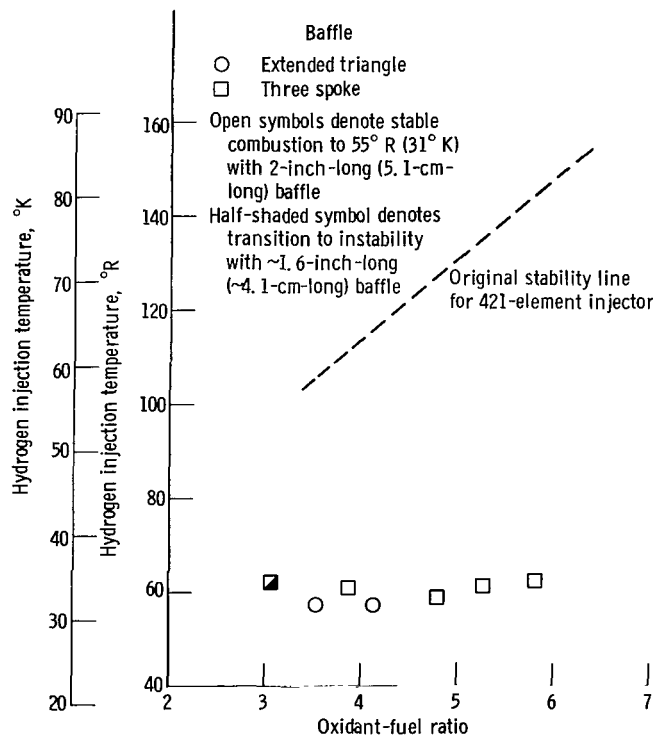


Figure 8. - Combustion stability with extended triangle and three-spoke injector face baffle configurations.

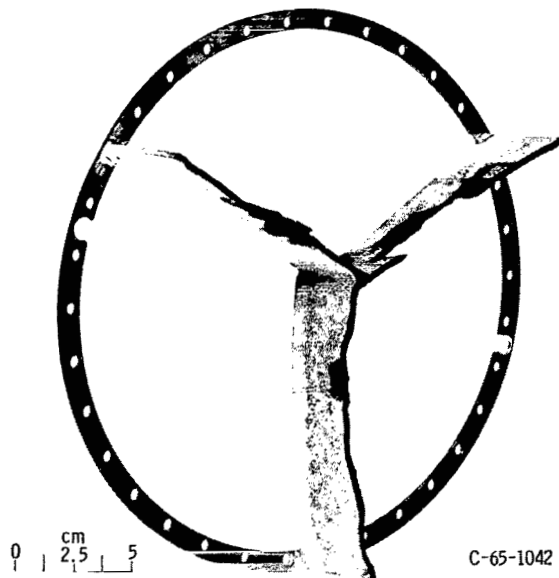


Figure 9. - Three-spoke baffle after instability was encountered due to shortened length.

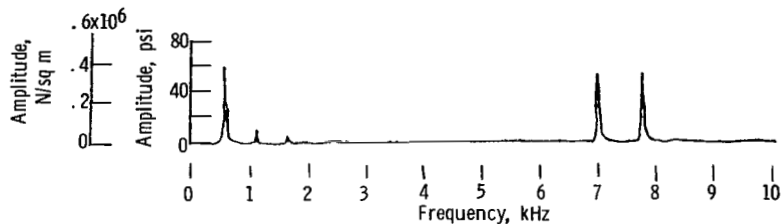


Figure 10. - Amplitude spectral density for three-spoke baffle burned to average length of 1.6 inches (4.1 cm). Oxidant-fuel ratio; 3.05; characteristic exhaust velocity efficiency, 93.3 per cent; amplitude, peak to peak.

Effect of Baffle Length with Four-Spoke Baffle

Figure 11 shows the effect of baffle length on combustion instability with a four-radial-spoke injector face baffle configuration (fig. 3(c)). No combustion instability was encountered with the 2-inch-long (5.1-cm-long) four-spoke configuration when it was operated down to the minimum hydrogen injection temperature limit of the facility. Figure 11 indicates stable operation at 59° R (33° K) over the oxidant-fuel range of 2.9 to 6.5.

A curve drawn through the four minimum stable hydrogen injection temperature data

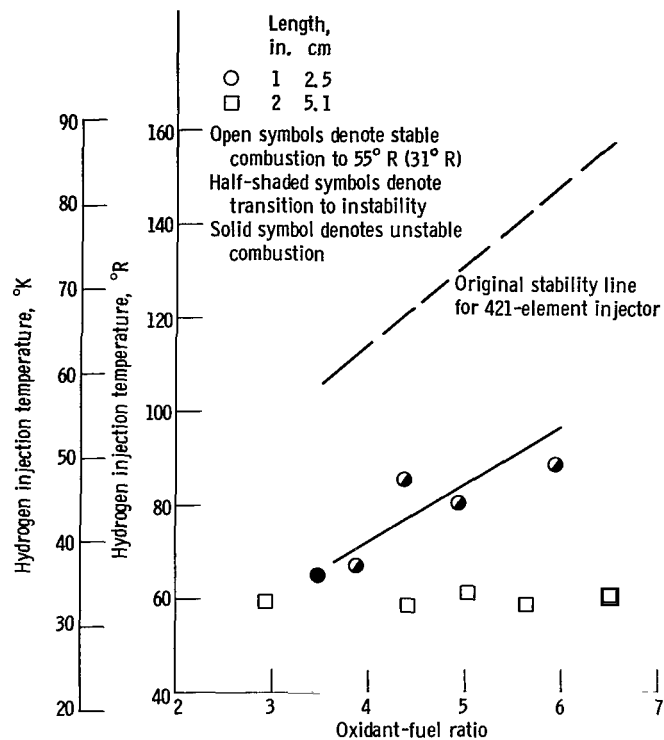


Figure 11. - Effect of baffle length on combustion stability limit with four-spoke baffle.

points (fig. 11) indicates that the 1 inch (2.5 cm) length is stable down to approximately 84° R (47° K) at an oxidant-fuel ratio of 5.0. One other test was not started at sufficiently high temperature to obtain transition to screech and is shown by the solid symbol in the figure to be unstable during the entire run at a temperature below the transition curve previously described. The amplitude spectral density for the 1-inch (2.5-cm) configuration is shown in figure 12 to have a screech frequency of 3200 hertz at an amplitude of 85 pounds per square inch (590 kN/sq m) peak-to-peak. This corresponds closely to the frequency of a first tangential mode in a bare chamber. The first Fourier harmonic is also shown in the figure. Amplitudes as large as 15 pounds per square inch (100 kN/sq m) at 5600 hertz were noted in some runs with this configuration. This is close to the third longitudinal mode.

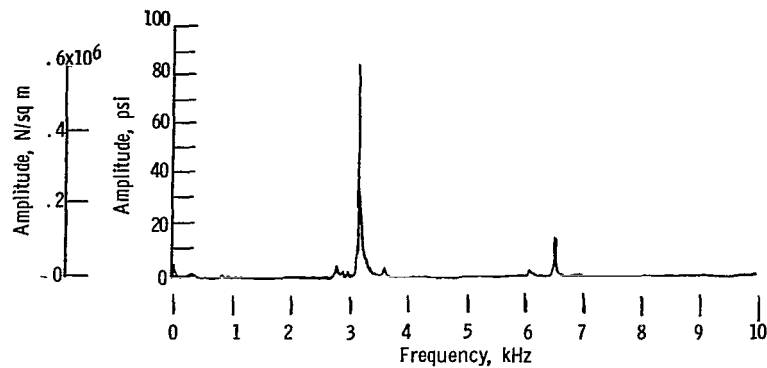


Figure 12. - Amplitude spectral density with 1-inch-long (2.5-cm-long) four-spoke baffle. Oxidant-fuel ratio, 5.93; characteristic exhaust velocity efficiency, 87.1 percent; amplitude, peak to peak.

Effect of Baffle Length with Seven-Spoke Baffle

The effect of baffle length on stability with a seven-radial-spoke configuration (figs. 3(a) and (c)) is demonstrated in figure 13, which shows the hydrogen injection temperature at the instant of transition to acoustic instability as a function of oxidant-fuel ratio. This figure shows that the transition points, while operating the modified injector (fig. 2(a)), establish a stability limit line 10^0 lower than the limit for the basic configuration at the same oxidant-fuel ratio of 5.0. Not only is the stability limit of the modified configuration about the same as that of the basic injector, but reference to figure 14(a) indicates that the amplitude spectral density is also about the same.

The 2-inch-long (5.1-cm-long) baffle (fig. 3(c)) provided stable operation down to the minimum temperature limit of the test facility (fig. 13). Tests were conducted at 54°R (30°K) over the oxidant-fuel ratio range of 3.6 to 5.9.

Operation with the 1 inch (2.5 cm) length (figs. 3(a) and (c)) was stable above 57°R (32°K) at an oxidant-fuel ratio of 4.0 and above 59°R (33°K) at 6.3. The screech that occurred was intermittent - changing from approximately 3000 hertz to a low frequency and back again in bursts of from 0.2 to 0.4 second. Although the 1 inch (2.5 cm) length improved the stability by reducing the minimum stable temperature an additional 25°R (14°K) below that for the $1/2$ inch (1.3 cm) length, the amplitudes were greater after transition. Figure 14 shows the amplitude spectral density for this configuration during instability. The instability occurred at 2800 hertz (amplitude, 135 psi (930 kN/sq m)) and at 3000 hertz (amplitude, 70 psi (480 kN/sq m)). First and second Fourier harmonics are evident. These frequencies are only slightly lower than the first tangential mode frequencies (they do not correspond to any acoustic mode predicted by bare chamber acoustic considerations).

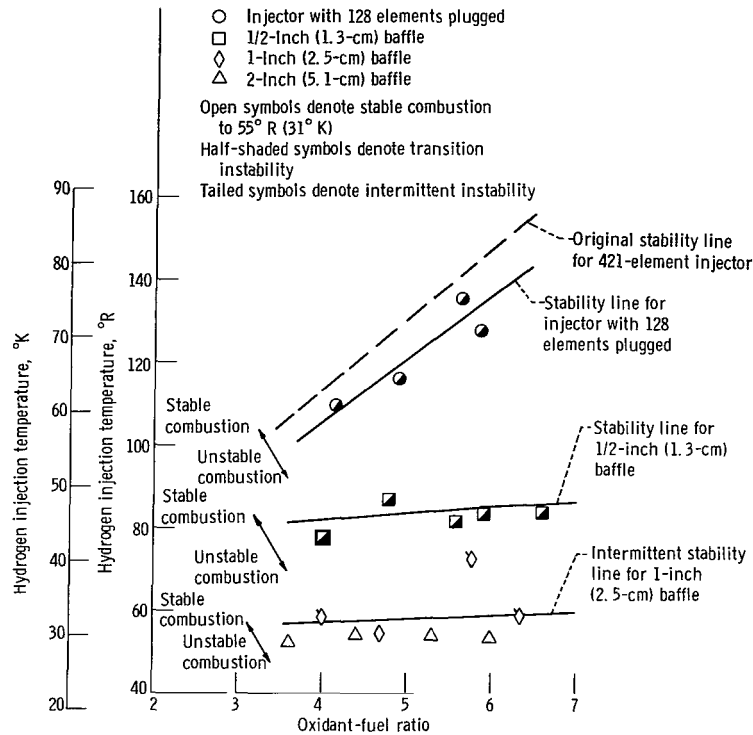


Figure 13. - Effect of baffle length on combustion stability limit with seven-spoke baffle.

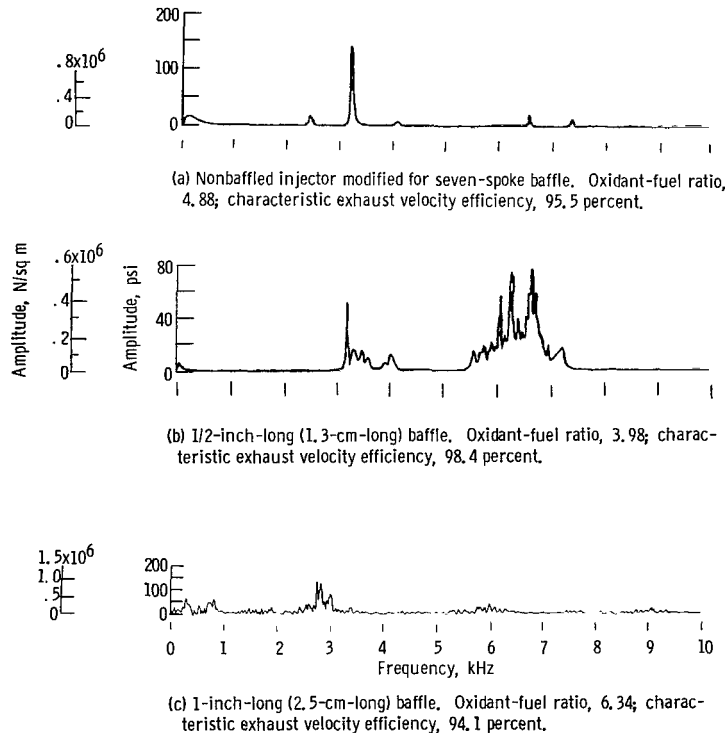


Figure 14. - Effect of length on amplitude spectral density with seven-spoke baffle. Unstable combustion; amplitude, peak to peak.

Hefner (ref. 15) has reported that when baffles are installed there is a noticeable frequency shift of a given mode of instability to a lower frequency at a rate of approximately 9 percent per inch of baffle length. The data from the Lewis Research Center tests indicate a trend similar to that of reference 15 but were too inconsistent to report a definite correlation.

Operation with the 1/2-inch-long (1.3-cm-long) baffle (fig. 3(c)) resulted in a minimum stable temperature of 81° R (45° K) at an oxidant-fuel ratio of 4.0 and 85° R (47° K) at 6.5. Figure 13 shows that at an oxidant-fuel ratio of 5.0, the stability limit was suppressed 48° R (27° K) below the corresponding limit for the basic injector and 38° R (21° K) below the corresponding limit for the modified injector. The amplitude spectral density with this configuration (fig. 14(b)) indicates that not only the stability limit but also the resulting amplitude of instability was much lower than with the basic injector. The amplitude of the first tangential mode was reduced from 150 to 50 pounds per square inch (1020 to 340 kN/sq m) peak-to-peak. There was, however, a broad band of instability between 5500 and 7200 hertz ranging in amplitude from 18 to 75 pounds per square inch (120 to 520 kN/sq m) peak-to-peak. Using bare chamber acoustics, these frequencies would correspond to second-tangential, second-tangential - first-longitudinal, first-radial, and/or second-tangential - second-longitudinal modes of instability.

Effect of Baffle Length with a Seven-Compartment Egg-Crate Baffle

The effect of baffle length on the combustion stability limits for an egg-crate baffle with approximately seven compartments is shown in figure 15. Operation with both the 1 $\frac{1}{4}$ inch and 2 inch (3.2 and 5.1 cm) lengths produced complete combustion stability down to the minimum temperature limit of the test facility.

The first test with the 1-inch-long (2.5-cm-long) configuration indicated a transition to screech at 93° R (52° K) at an oxidant-fuel ratio of 5.0. The solid data point shown in figure 15 represents unstable operation and was recorded as soon as nominal chamber pressure was established. Inspection of the baffle after the test revealed that it was burned back to an average length of approximately $\frac{1}{2}$ inch (1.3 cm) (fig. 16). It is not known whether or not any of this burning happened before the transition of the previous run. If some burning did occur early in the first run, it is possible that the transition point shown in figure 15 represents operation at some length less than 1 inch (2.5 cm), a fact that will have more significance in summary plots to be discussed later. Figure 17 indicates that the instability occurred at 3300 hertz and an amplitude of 55 pounds per square inch (380 kN/sq m) peak-to-peak.

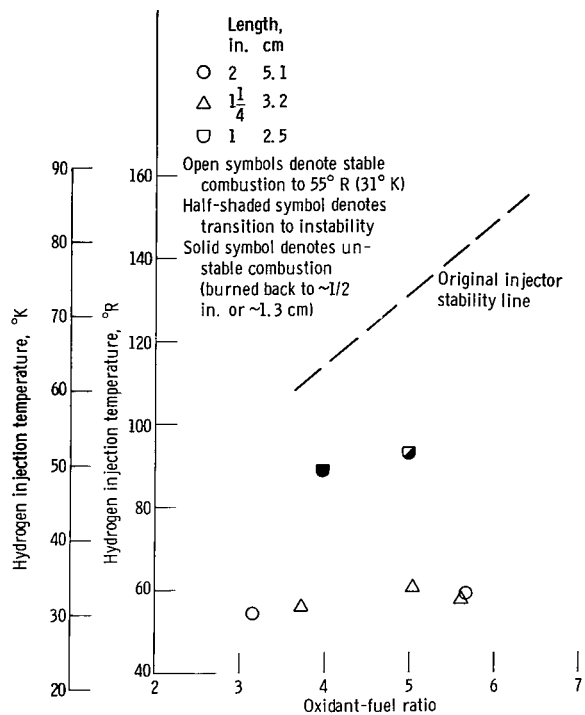


Figure 15. - Effect of baffle length on combustion stability limits with seven-compartment egg-crate baffle.

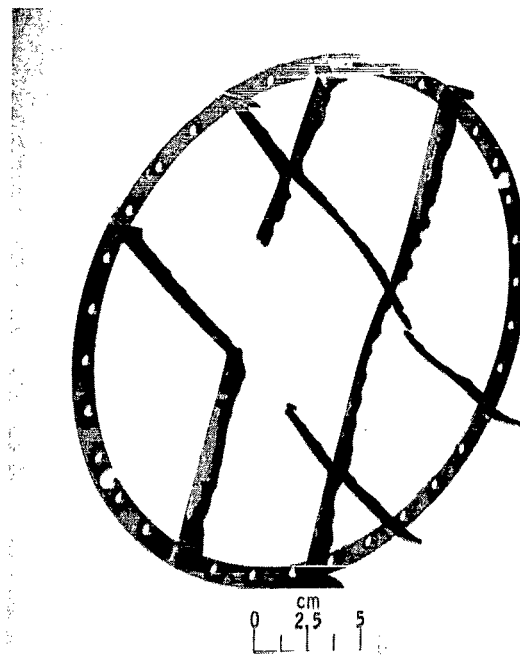


Figure 16. - 1-Inch-long (2.5-cm-long) seven-compartment egg-crate baffle after second run.

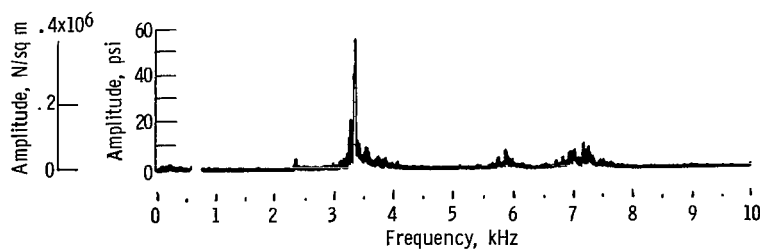


Figure 17. - Amplitude spectral density for 1-Inch-long (2.5-cm-long) seven-compartment egg-crate baffle. Oxidant-fuel ratio, 4.99; characteristic exhaust velocity efficiency, 94.0 percent; amplitude, peak to peak.

Effect of Baffle Length with a 25-Compartment Egg-Crate Baffle

The effect of baffle length on combustion stability limit using an egg-crate-type injector face baffle with approximately 25 compartments is presented in figure 18. Operation with the 1, $1\frac{1}{4}$, $1\frac{2}{3}$, and 2 inch (2.5, 3.2, 4.2, and 5.1 cm) lengths produced complete combustion stability down to the minimum temperature limit of the test facility. Instability was encountered with a $3/4$ inch (1.9 cm) length at a hydrogen injection temperature of 87°R (48°K) for an oxidant-fuel ratio of 5.0 (fig. 18). The minimum stable

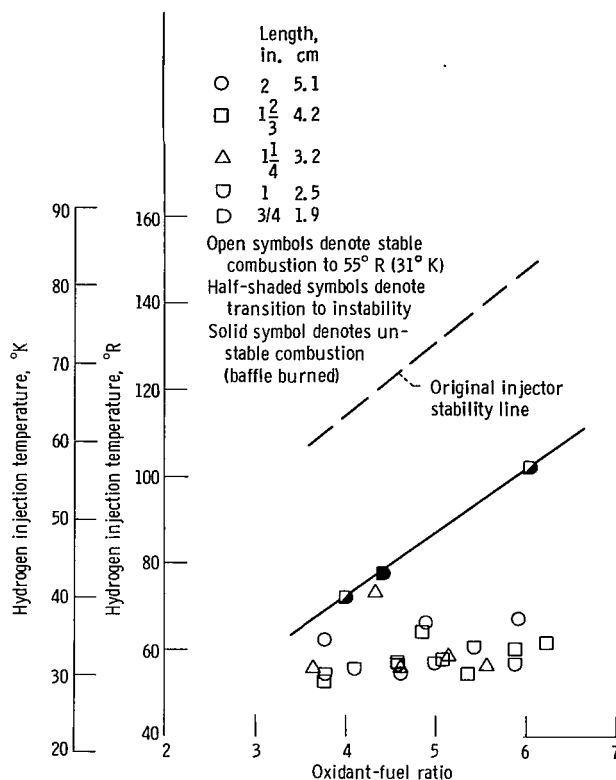


Figure 18. - Effect of baffle length on combustion stability limits with 25-compartment egg-crate baffle.

operating temperature was determined to be 71°R (39°K) at an oxidant-fuel ratio of 4.0 and 103°R (57°K) at 6.0. As indicated in figure 19, the instability occurred at 3200 hertz (first tangential mode) with an amplitude of 60 pounds per square inch (410 kN/sq m) peak-to-peak and at 6500 hertz with an amplitude of 30 pounds per square inch (210 kN/sq m) peak-to-peak; the latter, because of its relative amplitude, may be a second-tangential - second-longitudinal combined mode rather than a Fourier harmonic. Figure 18 also shows a data point that represents unstable operation and was recorded as soon as nominal chamber pressure was established during a third run with the $3/4$ -inch-

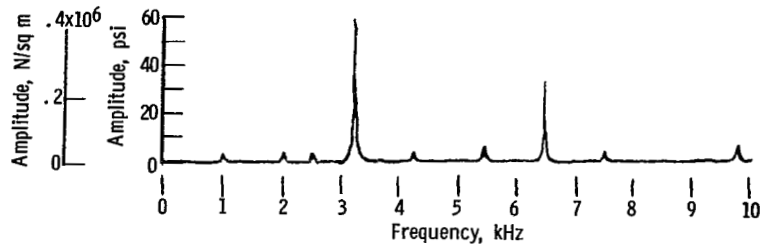


Figure 19. - Amplitude spectral density with 3/4-inch-long (1.9-cm-long) 25-compartment egg-crate baffle. Oxidant-fuel ratio, 3.99; characteristic exhaust velocity efficiency, 96.5 percent; amplitude, peak to peak.

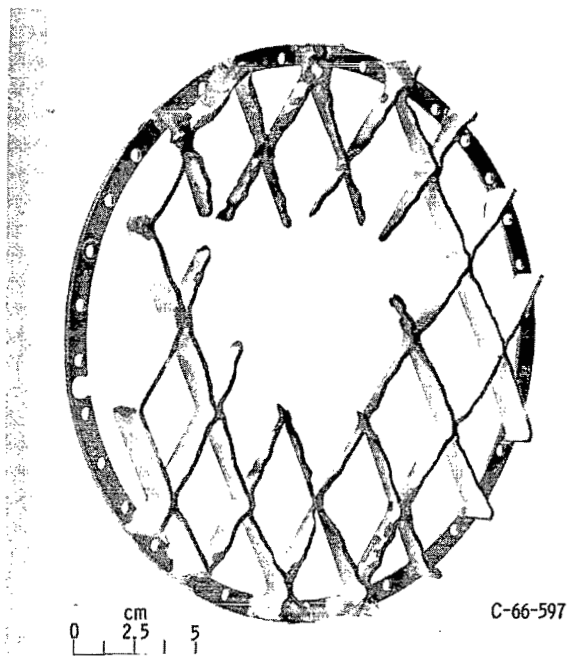


Figure 20. - 3/4-Inch-long (1.9-cm-long) 25-compartment egg-crate baffle after three unstable runs.

long (1.9-cm-long) configuration. Figure 20, taken after this run, shows the center portion of the baffle burned away and the outside still near the original 3/4 inch (1.9 cm) length. The difference in the stability of the burned and original configurations indicates that baffles are needed in the center of the injector as well as around the periphery even when the predominant mode of instability is tangential.

Effect of Baffle Length with 100-Compartment Egg-Crate Baffle

The effect of baffle length using an egg-crate-type injector face baffle with approxi-

mately 100 compartments (fig. 3(d)) is presented in figure 21. As with the other configurations presented, the 2 inch (5.1 cm) length produced stable operation to the temperature limit of the facility and over an oxidant-fuel ratio range of 4.0 to 8.2 (fig. 21). With a 1 inch (2.5 cm) length, two tests were stable below 60° R (33° K) and a third test was stable at 75° R (42° K). A fourth test went unstable at 77° R (43° K) with an oxidant-fuel ratio of 5.4. Figure 22 shows the amplitude of this single unstable test to be 20 and 18 pounds per square inch (140 and 120 kN/sq m) at frequencies of 2800 and 4600 hertz, respectively. A frequency of 2800 hertz does not correspond to any acoustic mode that would be expected in a bare chamber but may be the result of the frequency shift previously mentioned. The 4600 hertz could be a first-tangential - second-longitudinal combined mode. Because one test out of four was unstable, the 1 inch (2.5 cm) length was

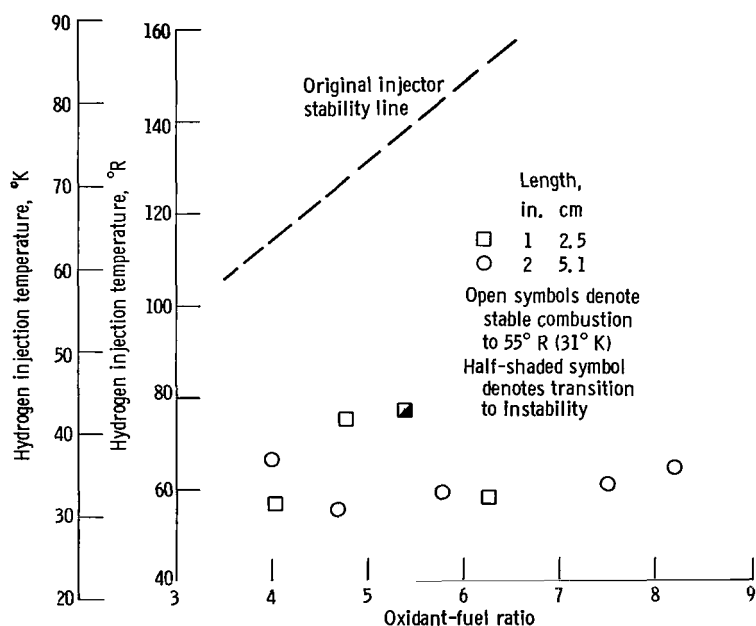


Figure 21. - Effect of baffle length on combustion stability limits with 100-compartment egg-crate baffle.

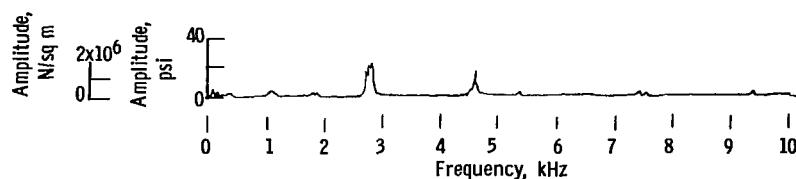


Figure 22. - Amplitude spectral density for 1-inch-long (2.5-cm-long) 100-compartment egg-crate baffle. Oxidant-fuel ratio, 4.03; characteristic exhaust velocity efficiency, 98.1 percent; amplitude, peak to peak.

defined as marginally stable. The baffle was inspected after four tests and was found to be in good condition. There were some heat marks on the baffle but only limited erosion at two locations near the chamber wall.

CORRELATIONS

Screech Amplitude

A summary of the peak-to-peak chamber pressure amplitude during screech with each baffle configuration that did not completely stabilize the combustor is shown in figure 23. The amplitudes are presented as a function of the corresponding minimum stable (transition) hydrogen injection temperature. When screech does occur with a baffled combustor, the amplitude decreases proportionally to the decrease in transition temperature. This trend was established without regard to baffle length or type. The exception

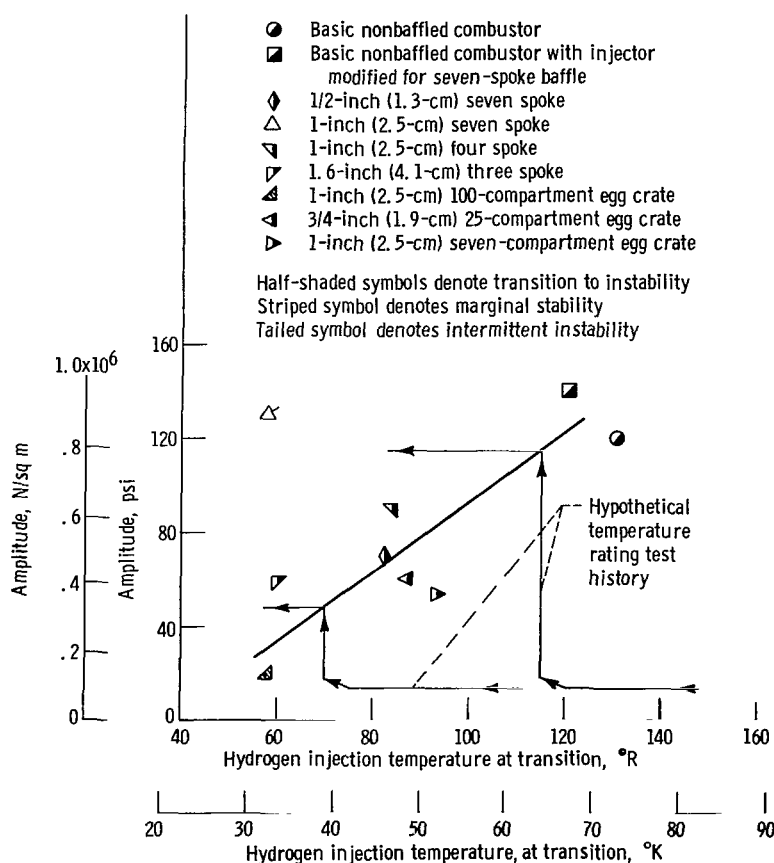


Figure 23. - Summary of effect of hydrogen injection transition temperature screech amplitude. Amplitude, peak to peak.

is the 1-inch-long (2.5-cm-long), seven-spoke baffle which was intermittently unstable. The amplitudes that are shown represent the magnitude of the largest spike in the frequency spectrum. Because these data were taken from individual tests, they are not at equivalent oxidant-fuel mixture ratios. The data are from the amplitude spectral density plots presented earlier. The individual amplitudes are typical for the respective baffles. The oxidant-fuel ratio variations could not be correlated with the small differences in amplitude observed with different runs.

Time histories of amplitude and hydrogen injection temperature during a ramp are shown in schematic form. At the start of a typical temperature rating test, the hydrogen injection temperature was greater than the transition value and the amplitude of the combustor noise was approximately 15 pounds per square inch (100 kN/sq m) peak-to-peak. As the temperature is decreased, the amplitude remains essentially constant with a slight increase near the transition temperature. The amplitude then steps to a higher value at the appropriate temperature but remains constant with further reduction of temperature. A similar trend of decreased amplitude with decreased transition temperature has been shown with unbaffled combustors (NASA unpublished data). The stability of a series of injectors with elements identical to those used with the baffle tests was altered by changing the injection mass flux distribution. The resulting amplitude followed the transition-temperature - amplitude trend of the baffled combustors. There was, therefore, no indication that the baffles were damping the amplitude of the established screech but were only altering the stability limit of the combustor. This change in stability limit resulted in a change in amplitude without regard for how the change was accomplished. In the case where the stability limit is altered by using an acoustic liner, there may also be an additional reduction in amplitude due to absorption of energy by the liner.

Combustion Performance

Characteristic exhaust velocity efficiency is shown as a function of hydrogen injection temperature in figure 24. The data are for stable operation with the basic injector. Stable operation at hydrogen injection temperatures less than 130° R (72° K) was obtained by using a perforated acoustic liner along the combustion chamber wall. The NASA experimental data are given in table III but are otherwise unpublished. All data are cross plots of characteristic exhaust velocity efficiency and hydrogen injection temperature at an oxidant-fuel ratio of 5.0. A list of these cross plotted data is presented in table IV.

The data form a band of $\pm 1\frac{1}{2}$ percent. This band is then extrapolated from 84° to 55° R (47° to 31° K). The shape of the curve is similar to that of the curves in refer-

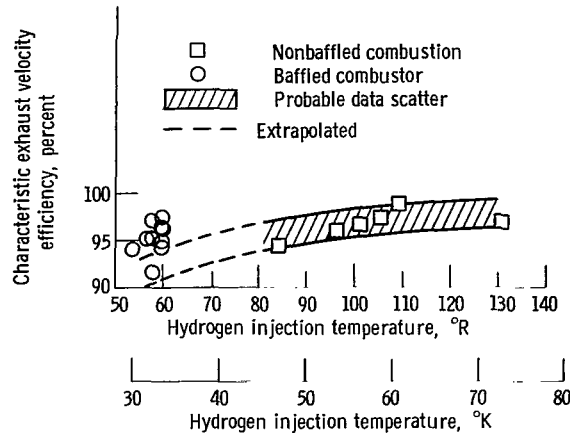


Figure 24. - Comparison of characteristic exhaust velocity efficiency with several injector face baffles to nonbaffled combustor at corresponding hydrogen injection temperatures. Data are for stable combustion and are cross plots at oxidant-fuel ratio of 5.0.

ence 16, which show a loss in combustion performance with decreasing hydrogen injection temperatures.

Also shown in figure 24 is the characteristic exhaust velocity efficiency of each baffle configuration. The data are cross plots at an oxidant-fuel ratio of 5.0 (table IV) and represent those baffles which produced stable operation at the minimum temperature limit of the test facility. Even if the combustion performance were extrapolated so as not to decrease with decreasing hydrogen injection temperature, operation with uncooled baffles would produce combustion performance at least equal to that of the nonbaffled combustor. However, flight engines with long run times would require some type of coolant for the baffles. If a dump-cooled technique were used, some penalty in combustion performance could be expected. Of the 11 baffles that were stable to the minimum temperature limit of the test facility, nine produced combustion performance higher than the extrapolated performance base line. The baffles may shelter the combustion zone and prevent crossflows or recirculation winds from causing off-mixture ratio pockets. The result is better combustion performance.

Combustion Stability

Figure 25 compares the minimum stable hydrogen injection temperature for several 1-inch-long (2.5-cm-long) baffles. The geometric parameter selected to describe the individual baffled compartments was the maximum dimension across a single baffle

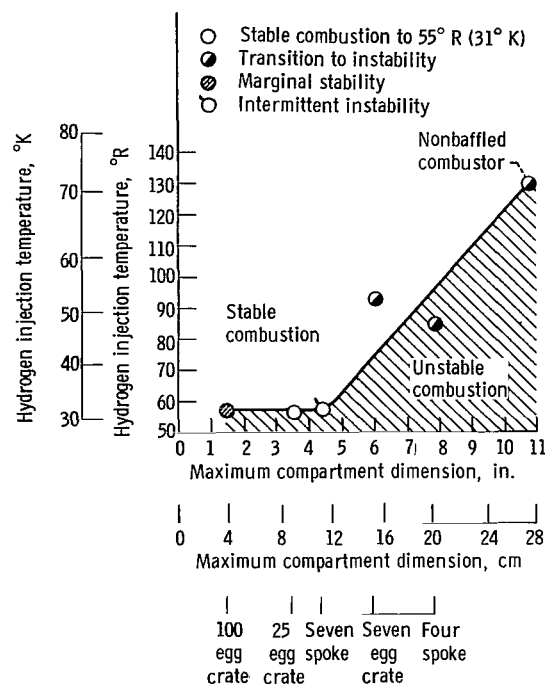


Figure 25. - Effect of maximum baffle compartment dimension on combustion stability limits with several 1-inch-long (2.5-cm-long) baffles. Oxidant-fuel ratio, 5.0.

cavity measured parallel to the injector face. For the case of dissimilar cavities (i. e., extended triangle) a weighted average based on the number of each cavity style was used. The sequential arrangement of the data using this parameter was not altered appreciably when other parameters (number of compartments, surface area to volume ratio, and baffle compartment area to combustor cross-sectional area) were used. The figure shows that, although rather constant stability is achieved with 1-inch-long (2.5-cm-long) baffles with maximum compartment dimensions between $1\frac{1}{2}$ and 4 inches (3.8 and 10.2 cm), the stability decreases with larger compartments. Screech occurs at increasingly higher injection temperatures for compartments larger than 4 inches (10.2 cm) across, approaching the stability limit of the nonbaffled combustor. As mentioned earlier, the transition data point of the seven-compartment egg-crate baffles may represent the stability limit for a baffle shorter than 1 inch (2.5 cm) in length and, therefore, would lie above the curve of figure 25. It can be seen from this figure that, for 1-inch-long (2.5-cm-long) baffles to be most effective, the maximum compartment dimension should not be greater than about 4 inches (10.2 cm).

Figure 26 correlates all of the data cross plotted to a mixture ratio of 5.0 by comparing combustion stability limits on a plot of baffle length as a function of maximum

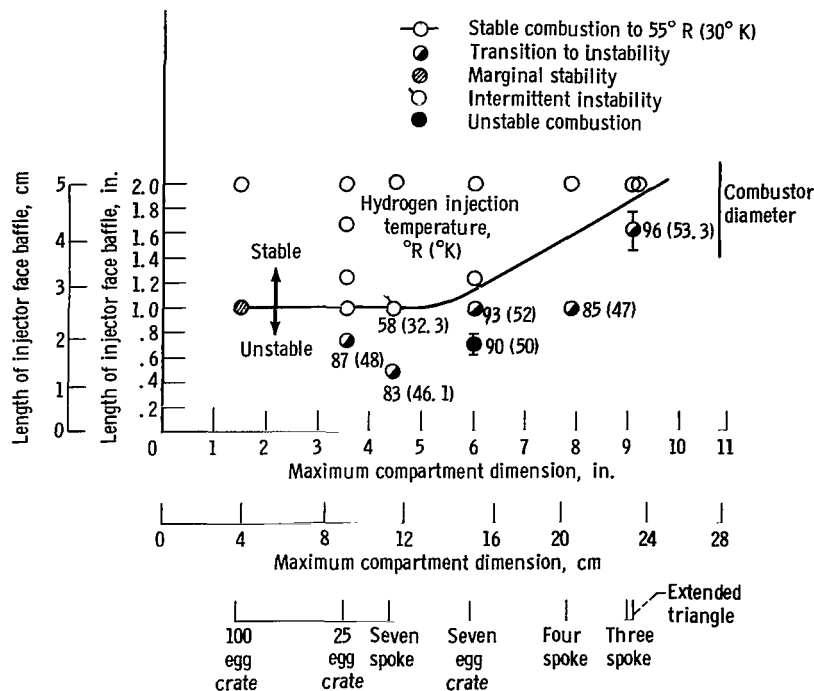


Figure 26. - Correlation of baffle length and maximum compartment dimension. Oxidant-fuel ratio, 5.0.

compartment dimension. The configurations that were stable to the minimum hydrogen injection temperature limit of the facility (55° R or 31° K) are shown above the curve. For a maximum compartment dimension of less than about 5 inches (12.7 cm), a baffle length of 1 inch (2.5 cm) will provide stable operation down to 55° R (31° K). The corresponding hydrogen injection temperature is shown with each data point. Curves of constant stability at temperatures other than 55° R (31° K) would have a shape similar to the one shown in this figure as is indicated by the data in the 80° to 90° R (44° to 50° K) range. Figures 25 and 26 both indicate that decreasing the maximum cavity dimension improves stability for cavities greater than 5 inches (12.7 cm) across but that further decreases produce no change in combustion stability.

One hypothesis as to why there is a marked change in the stabilizing effect of injector face baffles with maximum compartment dimensions above 4 inches (10.2 cm) deals with the sheltering afforded to the propellant streams during sensitive burning processes. The sensitivity of a vaporization rate controlling combustion process to a pressure disturbance has been shown in references 17 and 18 and indicates that the interaction may grow into combustion instability.

Streak photographs showed that, for the hydrogen - liquid-oxygen combustor, the combustion was completed 2 to 3 inches (5.1 to 7.6 cm) from the injector face. The most sensitive part of the combustion zone seemed to be the first inch. If the sensitive

region could be shielded from pressure disturbances inherently present in the combustor, there would be no opportunity for these disturbances to trigger instability.

Injector face baffles may provide shelter for the propellant streams by a mechanism similar to that described in reference 19, with flameholders for ramjet engines. These tests were conducted by moving propane and air at 75° F (297° K) past several recessed flameholders at varying velocities and mixture ratios. When a wall flameholder is used to stabilize a flame in a combustion gas stream, separation of the boundary layer occurs near the leading edge of the recessed contour in the wall, creating a pocket of recirculating gases. Hot gases in the recess ignite the adjacent fresh mixture in the flow stream and initiate a flame front. Therefore, if a flameholder is effective, the stream must recirculate into the cavity. Reference 19 measured the width of the cavity (parallel to stream flow) necessary to allow recirculation as a function of cavity depth. This length, defined as recirculation length, was essentially constant for variations in flow stream velocity and mixture ratio and was five times the recess depth. Consequently, if the width of a recess is more than five times the depth, the flow stream will recirculate into the cavity. If the width is less than five times the depth, the gases in the cavity will remain essentially stagnant.

If this mechanism were applied to figure 26, a 1-inch-long (2.5-cm-long) baffle should protect the propellant streams from velocity disturbances in the combustor when the maximum cavity dimension (recirculation length) is less than 5 inches (12.7 cm). Longer baffles should be required to provide equivalent shelter if the maximum cavity dimension is greater than 5 inches (12.7 cm). The correctness of this hypothesis depends on the validity of two assumptions: (1) that cross winds or pressure perturbations do exist parallel to the injector face and (2) that cavities with propellant streams issuing from the bottom have recirculation lengths analogous to those presented in reference 19.

The data acquired during this injector face baffle program may also be associated with the number of baffle compartments. This type of correlation would only be of value for 10.77-inch-diameter (27.4-cm-diam.) combustors, however, because it would not contain any information about the size of the combustor or about the size of the compartments.

If the data are compared with the models for baffle effectiveness, it is impossible to decide which model is more valid. The important point is that each model suggests using a large number of baffle compartments to improve stability. This design would provide a large surface area for viscous and thermal losses; it would obstruct pressure disturbances; and it would shelter the combustion process from cross velocities.

CONCLUDING REMARKS

Experimental tests were conducted at the Lewis Research Center to assess the worth of injector face baffles as screech suppression devices. The tests were conducted at a chamber pressure of 300 pounds per square inch absolute (2070 N/sq m), a combustor diameter of 10.77 inches (27.4 cm), a contraction ratio of 1.9, and a chamber length of 17.94 inches (45.6 cm) with injectors of 48 pounds (22 kg) thrust per element; the following results were obtained:

1. Injector face baffles 2 inches (5.1 cm) long produced stable operation down to 55° R (31° K) with as few as three baffle compartments.
2. Stability characteristics of several baffle configurations could be correlated with the maximum dimension in a single baffle compartment.
3. Injector face baffles 1 inch (2.5 cm) long produced marginal stability down to 55° R (31° K) when the maximum baffle cavity dimension was less than 5 inches (12.7 cm).
4. There was no loss of characteristic exhaust velocity efficiency when the combustor was stabilized with uncooled baffles.
5. When screech did occur with a baffled combustor, the amplitude decreased in proportion to the decrease in minimum stable hydrogen injection temperature.

Lewis Research Center,
National Aeronautics and Space Administration,
Cleveland, Ohio, November 22, 1967,
128-31-06-05-22.

REFERENCES

1. Nord, W. J., ed.: Analytical Model. Vol. 3 of Gemini Stability Improvement Program (Gemsip). Rep. No. GEMSIP-FR-1 (AFSSD-TR-66-2, DDC No. AD-626766), Aerojet-General Corp., Aug. 31, 1965.
2. Reardon, F. H.: M-1 Thrust Chamber Transverse Mode Combustion Stability Analysis. Rep. No. TCR 9621-012, Aerojet-General Corp., Apr. 1963.
3. Weiber, Paul R.: Acoustic Decay Coefficients of Simulated Rocket Combustors. NASA TN D-3425, 1966.
4. Reardon, F. H.; Crocco, L.; and Harrje, D. T.: Velocity Effects in Transverse Mode Liquid Propellant Rocket Combustion Instability. AIAA J., vol. 2, no. 9, Sept. 1964, pp. 1631-1641.

5. Wanhainen, John P.; Parish, Harold C.; and Conrad, E. William: Effect of Propellant Injection Velocity on Screech in 20,000-Pound Hydrogen-Oxygen Rocket Engine. NASA TN D-3373, 1966.
6. Senneff, John M.; and Morgante, Paul J.: Combustion Stability Investigation of the LEM Ascent Engine. Second Combustion Conference, Interagency Chemical Rocket Propulsion Group. Vol. I. Thomas W. Christian, ed. Rep. No. CPIA Publ. -105, Applied Physics Lab., Johns Hopkins Univ., May 1966, pp. 23-46. (Available from DDC as AD-484561.)
7. Ladd, J. W.: A Durable and Reliable Test Stand System for High-Accuracy Temperature Measurements in Cryogenic Ranges of Liquid Hydrogen and Liquid Oxygen. Advances in Cryogenic Engineering. Vol. 6. K. D. Timmerhaus, ed., Plenum Press, 1961, pp. 388-395.
8. Herr, Austin C.; Terbeek, Howard G.; and Tiefferman, Marvin W.: Suitability of Carbon Resistors of Field Measurements of Temperatures in Range of 35° to 100° R. NASA TN D-264, 1960.
9. Clayton, R. M.; and Rogero, R. S.: Experimental Measurements on a Rotating Detonation-Like Wave Observed During Liquid Rocket Resonant Combustion. Rep. No. TR-32-788 (NASA CR-67259). Jet Propulsion Lab., Calif. Inst. Tech., Aug. 15, 1965.
10. Huff, Vearl N.; Fortini, Anthony; and Gordon, Sanford: Theoretical Performance of JP-4 Fuel and Liquid Oxygen as a Rocket Propellant. II - Equilibrium Composition. NACA RM E56D23, 1956.
11. Gordon, Sanford; and McBride, Bonnie J.: Theoretical Performance of Liquid Hydrogen with Liquid Oxygen as a Rocket Propellant. NASA Memo 5-21-59E, 1959.
12. Crocco, Luigi; and Cheng, Sin-I: Theory of Combustion Instability in Liquid Propellant Rocket Motors. Butterworth Scientific Publ., 1956.
13. Wenzel, Leon M.; and Szuch, John R.: Analysis of Chugging in Liquid-Bipropellant Rocket Engines Using Propellants with Different Vaporization Rates. NASA TN D-3080, 1965.
14. Wanhainen, John P.; Antl, Robert J.; Hannum, Ned P.; and Mansour, Ali H.: Throttling Characteristics of a Hydrogen-Oxygen, Regeneratively Cooled, Pump-Fed Rocket Engine. NASA TM X-1043, 1964.

15. Hefner, R. J. : A Review of the Combustion Dynamics Aspects of the Gemini Stability Improvement Program. Second Combustion Conference, Interagency Chemical Rocket Propulsion Group. Vol. I. Thomas W. Christian, ed. Rep. No. CPIA Publ. -105, Applied Physics Lab. , Johns Hopkins Univ. , May 1966, pp. 13-22. (Available from DDC as AD-484561.)
16. Hannum, Ned P. ; and Conrad, E. William: Performance and Screech Characteristics of a Series of 2500-Pound-Thrust-Per-Element Injectors for a Liquid-Oxygen - Hydrogen Rocket Engine. NASA TM X-1253, 1966.
17. Priem, Richard J. ; and Guentert, Donald C. : Combustion Instability Limits Determined by a Non-Linear Theory and a One-Dimensional Model. NASA TN D-1409, 1962.
18. Mickelsen, William R. : Effect of Standing Transverse Acoustic Oscillations on Fuel-Oxidant Mixing in Cylindrical Combustion Chambers. NACA TN-3983, 1957.
19. Povinelli, L. A. : The Ignition Delay Concept for Recessed Flameholders. Combustion and Flame, vol. 4, no. 4, Dec. 1960, pp. 355-356.

TABLE I. - INJECTOR SPECIFICATIONS

Type of injector	Number of elements		Diameter of elements				Area of elements			
	O ₂	H ₂	O ₂		H ₂		O ₂		H ₂	
			in.	cm	in.	cm	in.	cm	in.	cm
Base line	421	421	0.052	0.1321	0.172	0.4368	0.894	2.27	4.616	11.72
Modified seven-spoke	293	293	.052	.1321	.172	.4368	.622	1.58	3.212	8.158
Modified four-spoke	339	339	.052	.1321	.172	.4368	.720	1.83	3.717	9.441

TABLE II. - BAFFLE CONFIGURATIONS TESTED

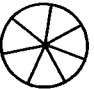
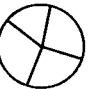


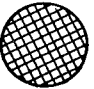
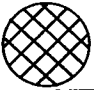

Type of injector		Length, in. (cm)					
		2(5.1)	1 $\frac{2}{3}$ (4.2)	1 $\frac{1}{4}$ (3.2)	1(2.5)	$\frac{3}{4}$ (1.9)	$\frac{1}{2}$ (1.3)
		Number of hot tests					
	Seven-spoke	4	---	---	4	---	5
	Four-spoke	5	---	---	5	---	---
	Three-spoke	5	---	---	---	---	---
	Extended triangle	2	---	---	---	---	---
	100-Compartment egg crate	5	---	---	4	---	---
	25-Compartment egg crate	4	6	5	6	3	---
	Seven-compartment egg crate	2	---	3	2	---	---

TABLE III. - EXPERIMENTAL DATA

Injector face baffle	Length		Hydrogen injection temperature		Oxidant-fuel ratio	Characteristic exhaust velocity efficiency, percent	Chamber pressure		Hydrogen flow rate, W_{H_2}		Oxygen flow rate, W_{O_2}	
	in.	cm	$^{\circ}R$	$^{\circ}K$			psi	kN/sq m	lb/sec	kg/sec	lb/sec	kg/sec
Base line	----	----	125.0	69.4	5.07	98.6	312.0	2.151×10^6	10.02	4.54	50.83	23.06
			123.0	68.3	4.51	98.8	302.0	2.082	10.64	4.83	48.01	21.78
			155.0	86.1	5.90	97.5	313.0	2.158	9.22	4.18	54.41	24.68
			88.0	48.9	4.19	98.5	303.0	2.089	11.07	5.02	46.47	21.08
			132.0	73.3	4.37	96.7	320.6	2.211	11.60	5.26	50.70	22.99
			122.0	67.8	4.06	97.7	313.4	2.161	11.80	5.35	48.00	21.77
			135.0	75	5.24	95.4	324.7	2.239	10.50	4.76	55.00	24.95
			153.0	85	7.30	94.8	280.4	1.933	7.40	3.36	54.00	24.49
			154.0	85.5	7.05	95.1	277.3	1.912	7.45	3.38	52.50	23.81
			145.0	80.5	6.51	94.3	282.5	1.948	8.03	3.64	52.30	23.72
			129.0	71.7	5.60	94.8	296.9	2.047	9.25	4.19	51.80	23.53
			136.0	75.6	4.60	95.8	299.0	2.062	10.69	4.85	49.20	22.32
			139.0	77.2	5.39	89.9	283.0	1.951	9.52	4.32	51.40	23.32
			137.0	76.1	5.06	90.1	279.0	1.924	9.79	4.44	49.50	22.45
			129.0	71.7	4.71	91.9	278.0	1.917	10.03	4.55	47.20	21.41
			129.0	71.7	4.99	93.1	273.0	1.882	9.34	4.24	46.60	21.14
Acoustic liner A	----	----	99.4	55.2	3.95	98.7	306	2.109×10^6	11.62	5.27	45.93	20.83
			103	57.2	5.0	97.6	306	2.109	9.95	4.51	49.79	22.58
			112.9	62.7	6.09	98.0	307	2.116	8.75	3.97	52.98	24.03
Acoustic liner B	----	----	90.5	50.3	3.97	97.0	305	2.103×10^6	11.72	5.32	46.58	21.13
			94.3	52.4	4.93	96.0	305	2.103	10.09	4.58	49.79	22.58
			107.0	59.4	5.98	98.0	306	2.107	8.80	3.99	52.69	23.90
Acoustic liner C	----	----	87.3	48.5	3.93	96.5	306	2.109×10^6	11.93	5.41	46.96	21.30
			103.0	57.2	4.93	97.0	307	2.116	10.09	4.58	49.78	22.58
			108.0	60.0	5.95	96.0	306	2.109	8.98	4.07	53.51	24.27
Acoustic liner D	----	----	86.5	48.10	3.89	95.9	305	2.103×10^6	12.14	5.51	47.22	21.42
			82.7	45.9	4.94	93.3	302	2.082	10.43	4.73	51.51	23.36
			83.3	46.3	5.90	92.5	300	2.068	9.29	4.21	54.83	24.87
Acoustic liner E	----	----	87.4	48.6	3.93	95.9	315	2.172×10^6	12.32	5.59	48.46	21.98
			96.9	53.83	5.02	95.6	313	2.158	10.37	4.70	52.00	23.59
			107.2	59.6	6.07	95.6	311	2.144	9.09	4.12	55.17	25.03
			91.9	51.10	4.49	96.2	314	2.165	11.15	5.06	50.08	22.72
			97.1	53.9	5.54	95.7	315	2.172	9.75	4.42	54.02	24.50
Acoustic liner F	----	----	84.03	46.7	3.94	96.9	308	2.123×10^6	11.94	5.42	47.07	21.35
			102.7	57.1	4.98	97.5	306	2.109	9.99	4.53	49.78	22.58
			109.6	60.7	5.99	97.5	308	2.123	8.92	4.05	53.46	24.25
			97.6	54.2	4.46	98.5	312	2.151	10.90	4.94	48.60	22.04
			108.6	60.3	5.62	97.9	310	2.137	9.31	4.22	52.31	23.73

TABLE III. - Continued. EXPERIMENTAL DATA

Injector face baffle	Length		Hydrogen injection temperature		Oxidant-fuel ratio	Characteristic exhaust velocity efficiency, percent	Chamber pressure		Hydrogen flow rate, W_{H_2}		Oxygen flow rate, W_{O_2}	
	in.	cm	$^{\circ}R$	$^{\circ}K$			psi	kN/sq m	lb/sec	kg/sec	lb/sec	kg/sec
Acoustic liner G	-----	-----	97.0	53.9	3.96	100.8	311	2.144×10^6	11.54	5.23	45.66	20.71
			107.9	59.9	4.82	99.9	308	2.123	10.02	4.55	48.26	21.89
			113.0	62.8	6.07	98.9	310	2.137	8.76	3.97	53.2	24.13
			111.2	61.8	4.49	99.0	308	2.123	10.62	4.82	47.67	21.62
			106.8	59.30	5.52	96.7	307	2.116	9.43	4.28	52.08	23.62
			105.8	58.8	4.24	98.6	307	2.116	11.08	5.03	47.00	21.32
Base line modified for seven spoke	-----	-----	116.2	64.6	4.88	95.5	303	2.089×10^6	10.37	4.70	50.65	22.97
			109.5	60.8	4.14	94.9	299	2.062	11.57	5.25	47.9	21.73
			128.0	71.1	5.85	93.9	303	2.089	9.36	4.25	54.7	24.81
			135.5	75.3	5.61	94.9	306	2.109	9.65	4.38	54.1	24.54
Seven spoke	2	5.1	54.0	30	4.40	94.4	281	1.937×10^6	10.50	4.76	46.2	20.96
			53.8	29.9	5.29	93.1	299	2.062	10.0	4.53	52.8	23.95
			52.4	29.1	3.60	95.8	292	2.014	12.4	5.62	44.7	20.27
			53.8	29.9	5.99	93.8	301	2.075	9.2	4.17	55.1	24.99
Seven spoke	1	2.5	54.6	30.3	4.69	92.6	306	2.109×10^6	11.0	4.99	51.6	23.41
			58.2	32.3	3.98	94.5	304	2.096	12.0	5.44	47.8	21.68
			58.9	32.7	6.34	94.1	309	2.131	9.0	4.08	56.9	25.81
			72.7	40.4	5.76	88.9	289	1.993	9.5	4.31	54.6	24.77
Seven spoke	$\frac{1}{2}$	1.3	86.8	48.2	4.77	98.6	337	2.323×10^6	11.4	5.17	54.6	24.77
			77.9	43.3	3.98	98.4	330	2.275	12.7	5.76	50.7	22.99
			83.3	46.3	5.90	96.7	313	2.158	9.4	4.26	55.4	25.13
			81.7	45.4	5.56	95.4	304	2.096	9.6	4.35	53.4	24.22
			83.8	46.6	6.59	94.0	302	2.082	8.7	3.95	57.3	25.99
Four spoke	2	5.1	61.3	34.1	5.03	95.8	319	2.199×10^6	10.8	4.89	54.2	24.58
			58.6	32.6	4.40	94.6	301	2.075	11.0	4.99	48.3	21.91
			58.8	32.7	5.63	93.9	313	2.158	9.7	4.39	54.9	24.90
			60.6	33.7	6.50	93.2	303	2.089	8.7	3.95	56.5	25.63
			59.6	33.1	2.91	95.8	301	2.075	14.7	6.67	42.8	19.41
Four spoke	1	2.5	65.5	36.4	3.42	98.0	300	2.068×10^6	12.8	5.81	43.7	19.82
			80.6	44.8	4.92	89.1	269.0	1.85	9.67	4.39	47.52	21.55
			67.2	37.3	3.86	89.5	288.0	1.986	13.22	5.99	47.18	21.40
			88.5	49.2	5.93	87.1	266.0	1.834	8.65	3.92	51.27	23.26
			85.5	47.5	4.36	92.9	277.0	1.909	10.41	4.72	45.36	20.57
Three spoke	2	5.1	58.9	32.7	4.78	93.3	317	2.186×10^6	11.0	4.99	52.9	23.99
			60.6	33.7	3.86	97.7	307	2.117	11.9	5.39	46.0	20.86
			62.8	34.9	5.81	94.4	312	2.151	9.5	4.31	55.2	25.04
			61.1	33.9	5.26	92.2	310	2.137	10.3	4.67	54.0	24.99

TABLE III. - Continued. EXPERIMENTAL DATA

Injector face baffle	Length		Hydrogen injection temperature		Oxidant-fuel ratio	Characteristic exhaust velocity efficiency, percent	Chamber pressure		Hydrogen flow rate, W_{H_2}		Oxygen flow rate, W_{O_2}	
	in.	cm	$^{\circ}R$	$^{\circ}K$			psi	kN/sq m	lb/sec	kg/sec	lb/sec	kg/sec
Three spoke	~1.6	~4.1	62.6	34.8	3.05	93.3	275	1.896×10^6	13.2	5.99	40.4	18.33
Extended triangle	2	5.1	57.8	32.1	3.53	92.8	297	2.047×10^6	12.8	5.81	45.4	20.59
			58.0	32.2	4.12	92.1	304	2.096	11.9	5.39	48.8	22.13
100-Compartment egg crate	2	5.1	64.8	36.0	8.20	87.3	244	1.682×10^6	6.6	2.99	53.8	24.40
			66.8	37.1	4.00	95.8	305	2.103	11.9	5.39	47.5	21.55
			55.6	30.9	4.68	97.8	327	2.255	11.2	5.08	52.1	23.63
			59.0	32.8	5.77	96.2	321	2.213	9.7	4.39	55.9	25.36
			61.0	33.9	7.50	96.6	303	2.089	7.8	3.54	58.1	26.35
100-Compartment egg crate	1	2.5	77.0	42.8	5.39	96.4	333	2.296×10^6	10.4	4.72	56.2	25.49
			75.3	41.8	4.77	99.3	337	2.323	11.1	5.03	53.0	24.04
			56.8	31.6	4.03	98.1	312	2.151	11.7	5.31	47.2	21.41
			58.1	32.3	6.25	96.6	318	2.192	8.9	4.04	55.8	25.31
25-Compartment egg crate	2	5.1	62.3	34.6	3.76	97.2	340	2.344×10^6	13.6	6.17	51.3	23.27
			66.6	37.0	4.88	96.0	316	2.179	10.7	4.85	52.2	23.68
			54.6	30.3	4.59	97.3	322	2.220	11.2	5.08	51.4	23.32
			67.2	37.3	5.91	96.1	318	2.193	9.5	4.31	56.0	25.40
			64.1	35.6	4.84	94.5	324	2.233	11.0	4.99	53.4	24.22
25-Compartment egg crate	$1\frac{2}{3}$	4.2	52.7	29.3	3.74	99.2	324	2.233×10^6	12.6	5.72	47.2	20.50
			54.7	30.4	5.34	97.7	325	2.240	10.0	4.53	53.5	24.27
			58.0	32.2	5.08	97.0	320	2.206	10.3	4.67	52.5	23.81
			60.1	33.4	5.87	97.5	330	2.275	9.6	4.35	56.6	25.67
			61.4	34.1	6.23	97.3	324	2.233	9.1	4.13	57.1	25.90
25-Compartment egg crate	$1\frac{1}{4}$	3.2	58.3	32.4	5.13	93.2	319	2.199×10^6	10.7	4.85	54.7	24.81
			56.0	31.1	4.60	96.0	307	2.117	10.7	4.85	49.4	22.41
			55.8	31.0	3.64	99.2	316	2.179	12.6	5.72	46.0	20.86
			56.3	31.3	5.57	96.5	308	2.124	9.4	4.26	52.5	23.81
			73.2	40.7	4.34	94.3	319	2.199	11.8	5.35	51.4	23.32
25-Compartment egg crate	1	2.5	60.6	33.7	5.41	91.6	305	2.102×10^6	10.0	4.53	54.0	24.49
			57.0	31.7	4.57	95.3	307	2.117	10.8	4.89	49.5	22.45
			55.6	30.9	4.09	95.4	299	2.062	11.4	5.17	46.5	21.09
			57.0	31.7	4.99	96.5	291	2.006	9.5	4.31	47.4	21.50
			54.3	30.2	3.76	98.2	343	2.365	13.4	6.08	50.6	22.95
			56.9	31.6	5.87	94.6	320	2.206	9.6	4.35	56.4	25.58

TABLE III. - Concluded. EXPERIMENTAL DATA

Injector face baffle	Length		Hydrogen injection temperature		Oxidant-fuel ratio	Characteristic exhaust velocity efficiency, percent	Chamber pressure		Hydrogen flow rate, W_{H_2}		Oxygen flow rate, W_{O_2}	
	in.	cm	$^{\circ}R$	$^{\circ}K$			psi	kN/sq m	lb/sec	kg/sec	lb/sec	kg/sec
25-Compartment egg crate	$\frac{3}{4}$	1.9	72.3	40.2	3.99	96.5	307	2.117×10^6	11.9	5.39	47.4	21.50
			102.6	57	6.04	98.1	307	2.117	8.8	3.99	53.4	24.22
			78	43.3	4.42	97.9	301	2.075	11.2	5.08	49.5	22.45
Seven-compartment egg crate	2	5.1	59.2	32.9	5.67	96.6	319	2.199×10^6	9.6	4.35	54.6	24.76
			54.4	30.2	3.15	98.3	306	2.109	13.8	6.26	43.3	19.64
Seven-compartment egg crate	$1\frac{1}{4}$	3.2	60.6	33.7	5.03	89.4	316	2.179×10^6	11.1	5.03	55.8	25.31
			55.9	31.1	3.73	94.4	301	2.075	12.4	5.62	46.1	20.91
			57.9	32.2	5.60	91.8	302	2.082	9.6	4.35	53.9	24.45
Seven-compartment egg crate	~1	~2.5	93.2	51.8	4.99	94.0	315	2.172×10^6	10.8	4.89	53.7	24.36
			89.3	49.6	3.97	92.4	321	2.213	13.1	5.94	52.0	23.59

TABLE IV. - CROSS PLOT AT OXIDANT-FUEL RATIO OF 5.0

Configuration	Length		Hydrogen injection temperature		Characteristic exhaust velocity efficiency, percent
	in.	cm	°R	°K	
Acoustic liner A	--	---	105	58.3	97.7
Acoustic liner B	--	---	98.5	54.7	97.3
Acoustic liner C	--	---	101	56.1	96.7
Acoustic liner D	--	---	84	46.7	94.2
Acoustic liner E	--	---	96.3	53.5	95.8
Acoustic liner F	--	---	101	56.1	97.6
Acoustic liner G	--	---	109	60.6	98.8
Seven spoke	2	5.1	54	30.0	94.0
Four spoke	2	5.1	60	33.3	94.7
Three spoke	2	5.1	60	33.3	94.2
Extended triangle	2	5.1	58	32.2	91.7
100-Compartment egg crate	2	5.1	60	33.3	96.3
25-Compartment egg crate	2	5.1	60	33.3	96.5
↓	$1\frac{2}{3}$	4.2	60	33.3	97.5
	$1\frac{1}{4}$	3.2	58	32.2	95.2
	1	2.5	57	31.7	95.2
	1	2.5	58	32.2	97.2
Seven-compartment egg crate	2	5.1	58	32.2	97.2
Seven-compartment egg crate	1	2.5	58	32.2	91.5

$\Gamma = \langle \Gamma_1, \Gamma_2 \rangle$ is a Γ -invariant \mathbb{R} -linear map from $\mathcal{H}^1(\Gamma_1, \mathbb{R}) \oplus \mathcal{H}^1(\Gamma_2, \mathbb{R})$ to $\mathcal{H}^1(\Gamma, \mathbb{R})$. The map Γ is called the *restriction map*. The map Γ is surjective if and only if Γ_1 and Γ_2 are Γ -invariant. The map Γ is called the *restriction map*. The map Γ is called the *restriction map*.

POSTMASTER: If Undeliverable (Section 158
Postal Manual) Do Not Return

"The aeronautical and space activities of the United States shall be conducted so as to contribute . . . to the expansion of human knowledge of phenomena in the atmosphere and space. The Administration shall provide for the widest practicable and appropriate dissemination of information concerning its activities and the results thereof."

—NATIONAL AERONAUTICS AND SPACE ACT OF 1958

NASA SCIENTIFIC AND TECHNICAL PUBLICATIONS

TECHNICAL REPORTS: Scientific and technical information considered important, complete, and a lasting contribution to existing knowledge.

TECHNICAL NOTES: Information less broad in scope but nevertheless of importance as a contribution to existing knowledge.

TECHNICAL MEMORANDUMS: Information receiving limited distribution because of preliminary data, security classification, or other reasons.

CONTRACTOR REPORTS: Scientific and technical information generated under a NASA contract or grant and considered an important contribution to existing knowledge.

TECHNICAL TRANSLATIONS: Information published in a foreign language considered to merit NASA distribution in English.

SPECIAL PUBLICATIONS: Information derived from or of value to NASA activities. Publications include conference proceedings, monographs, data compilations, handbooks, sourcebooks, and special bibliographies.

TECHNOLOGY UTILIZATION PUBLICATIONS: Information on technology used by NASA that may be of particular interest in commercial and other non-aerospace applications. Publications include Tech Briefs, Technology Utilization Reports and Notes, and Technology Surveys.

Details on the availability of these publications may be obtained from:

SCIENTIFIC AND TECHNICAL INFORMATION DIVISION
NATIONAL AERONAUTICS AND SPACE ADMINISTRATION

Washington, D.C. 20546